Plasma Properties in Giant Negative Ion Sources for Fusion

E Sartori[1,2], G. Serianni, P. Veltri, NBTF Team*

B Heinemann, C Wimmer, D Wűnderlich, U Fantz (Max-Planck-Institut für Plasmaphysik)
H Nakano, K Tsumori (National institute for Fusion Science)
H Tobari, M Kisaki, M Kashiwagi (National Institutes for Quantum and Radiological Science and Technology (QST))
D Bruno, F Taccogna (ISTP Bari)

* NBTF TEAM AS LISTED IN 2022 NUCL. FUSION 62 086022

[1)] *Consorzio RFX, Corso Stati Uniti 4, I-351, 27 Padova, Italy*
[2)] *Department of Management and Engineering, Università degli Studi di Padova, Strad. S. Nicola 3, 36100 Vicenza, Italy*
[3)] *ITER Organization*

ICIS'23 International Conference on Ion Sources
Victoria, BC, Canada

Giant negative ion sources for fusion

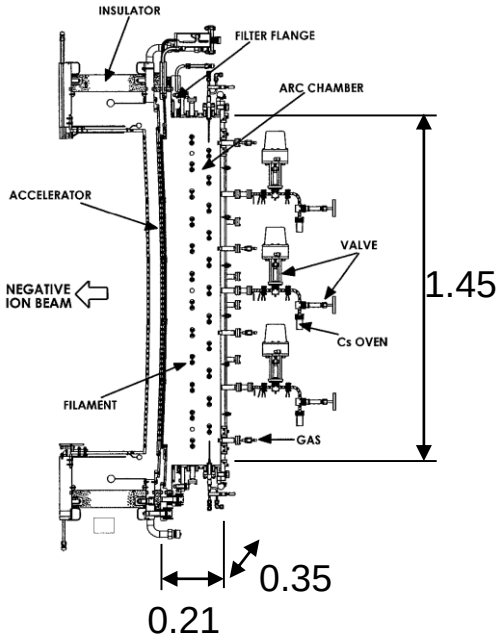

LHD H⁻ source

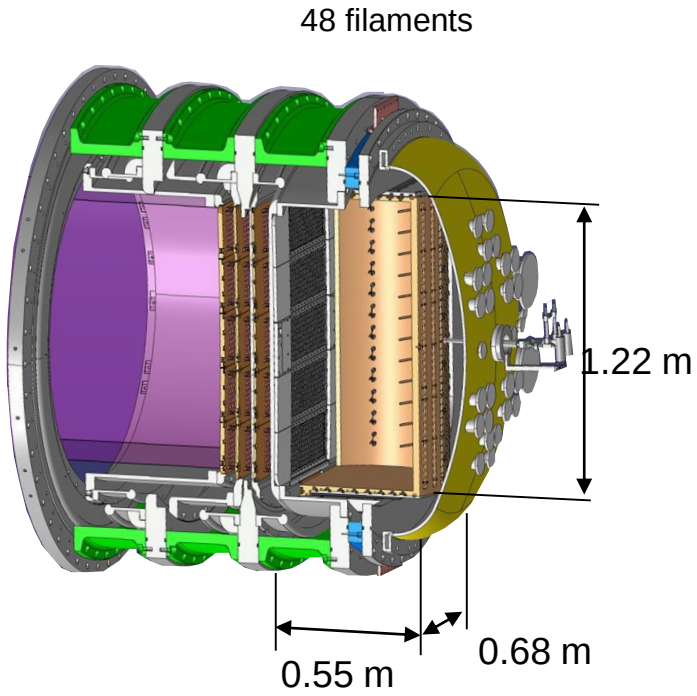

JT60SA H⁻ source

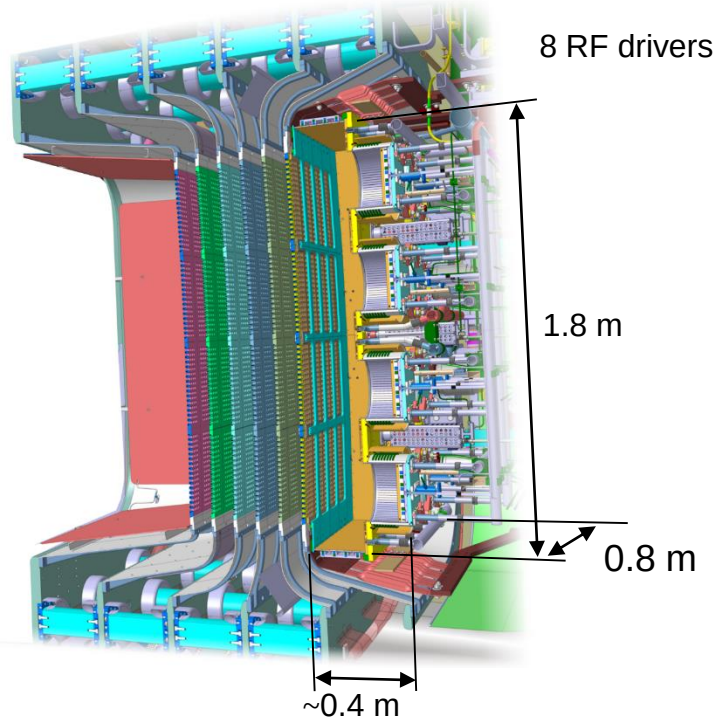

ITER H⁻⁻ source

	V (m^3)	A(m^2)	Deployment	Status
LHD H⁻⁻source	0.11	1.23	1998	Concluded
JT60SA H⁻ source	0.41	3.2	1996	Mature
ITER H⁻⁻ source	0.44	5.2	2025	Ongoing

Giant negative ion sources

ITER H- beam source
Requirements to deliver 17 MW per injector:

- for up to 1h, at 870/1000 keV for H^-/D^-
- low-divergence <7 mrad
- j_{ext} 330/285 A/m^2 of H^-/D^-
- low filling pressure of 0.3 Pa

Different discharge type: RF-driven to limit maintenance

Coordinated efforts towards ITER neutral beams
with physics and technological development
→ Community of giant NI sources
→ Neutral Beam Test Facility

MITICA (beam source at 1MeV) to begin first beam operations in 2025:
focus on ion source

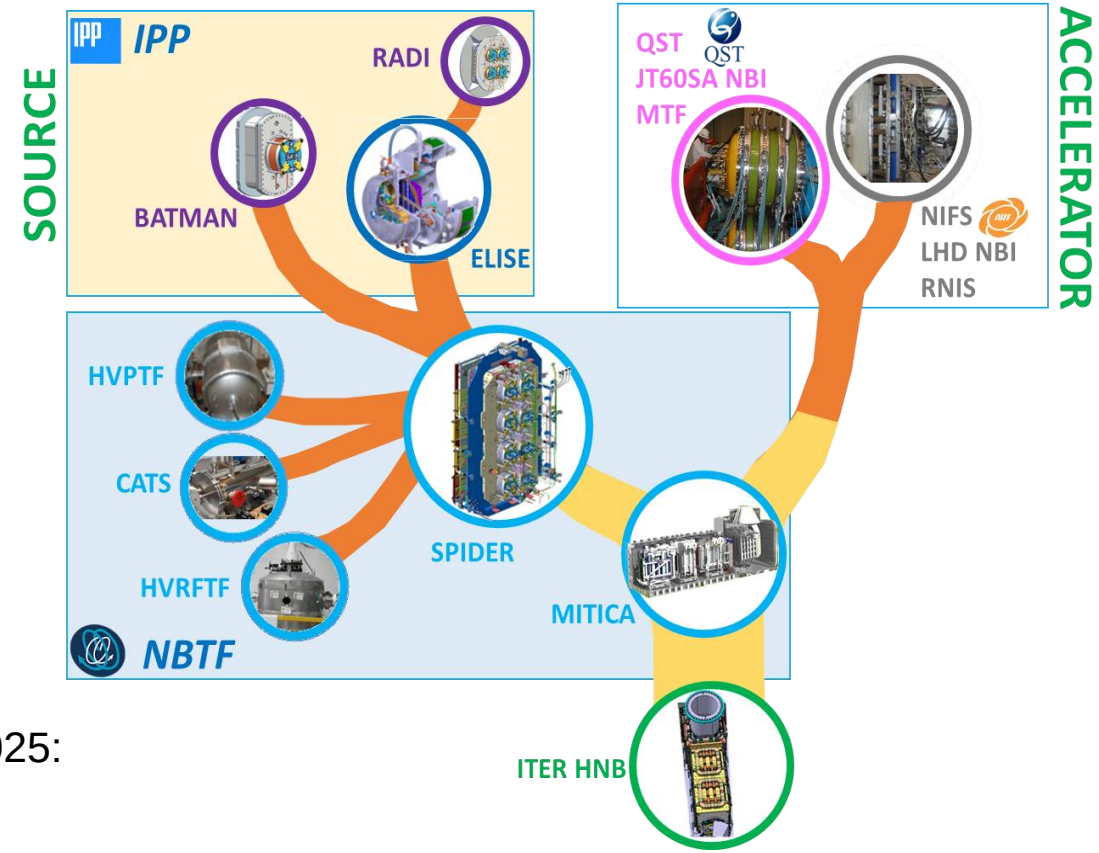

	V (m^3)	A(m^2)	Deployment	Status
LHD H$^-$source	0.11	1.23	1998	Concluded
JT60SA H$^-$ source	0.41	3.2	1996	Mature
ITER H$^-$ source	0.44	5.2	2025	Ongoing

Giant negative ion sources

ITER H- beam source
Requirements to deliver 17 MW per injector:

- for up to 1h, at 870/1000 keV for H^-/D^-
- low-divergence <7 mrad
- j_{ext} 330/285 A/m^2 of H^-/D^-
- low filling pressure of 0.3 Pa

Different discharge type: RF-driven to limit maintenance

Coordinated efforts towards ITER neutral beams
with physics and technological development
→ Community of giant NI sources
→ Neutral Beam Test Facility

MITICA (beam source at 1MeV) to begin first beam operations in 2025:
focus on ion source

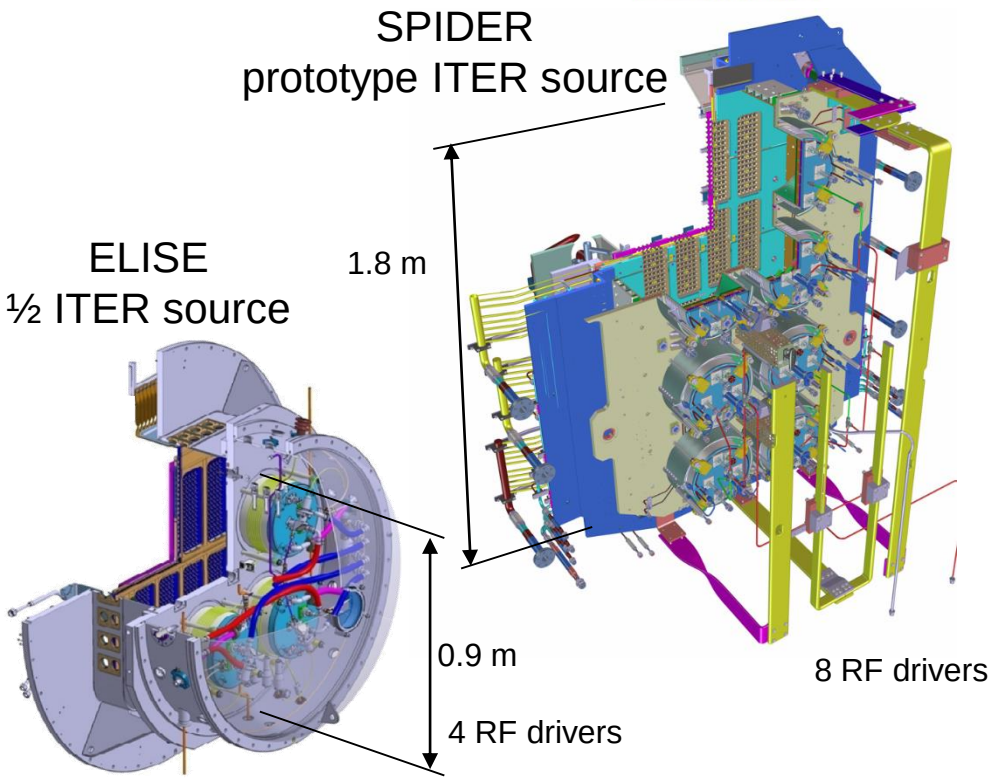

Test stands for the ITER H$^-$ source

	V (m^3)	A(m^2)	Started development	Status
LHD H$^-$source	0.11	1.23	1998	Concluded
JT60SA H$^-$ source	0.41	3.2	1996	Mature
1:1 source SPIDER **½ source ELISE**	0.44 0.24	5.2 2.9	2018 2013	Ongoing

Giant negative ion sources

ITER H- beam source
Requirements to deliver 17 MW per injector:

- for up to 1h, at 870/1000 keV for H^-/D^-
- low-divergence <7 mrad
- j_{ext} 330/285 A/m^2 of H^-/D^-
- low filling pressure of 0.3 Pa

Different discharge type: RF-driven to limit maintenance

Coordinated efforts towards ITER neutral beams
with physics and technological development
→ Community of giant NI sources
→ Neutral Beam Test Facility

MITICA (beam source at 1MeV) to begin first beam operations in 2025:
focus on ion source

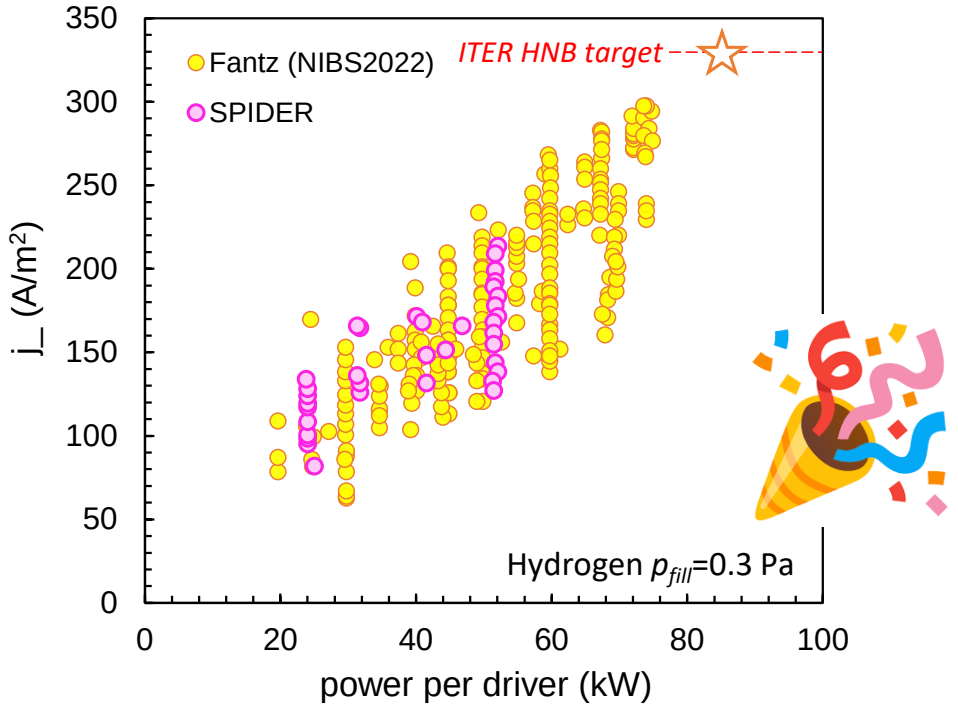

Test stands for the ITER H$^-$ source

	V (m^3)	A(m^2)	Started development	Status
LHD H$^-$source	0.11	1.23	1998	Concluded
JT60SA H$^-$ source	0.41	3.2	1996	Mature
1:1 source SPIDER **½ source ELISE**	0.44 0.24	5.2 2.9	2018 2013	Ongoing

Giant negative ion sources

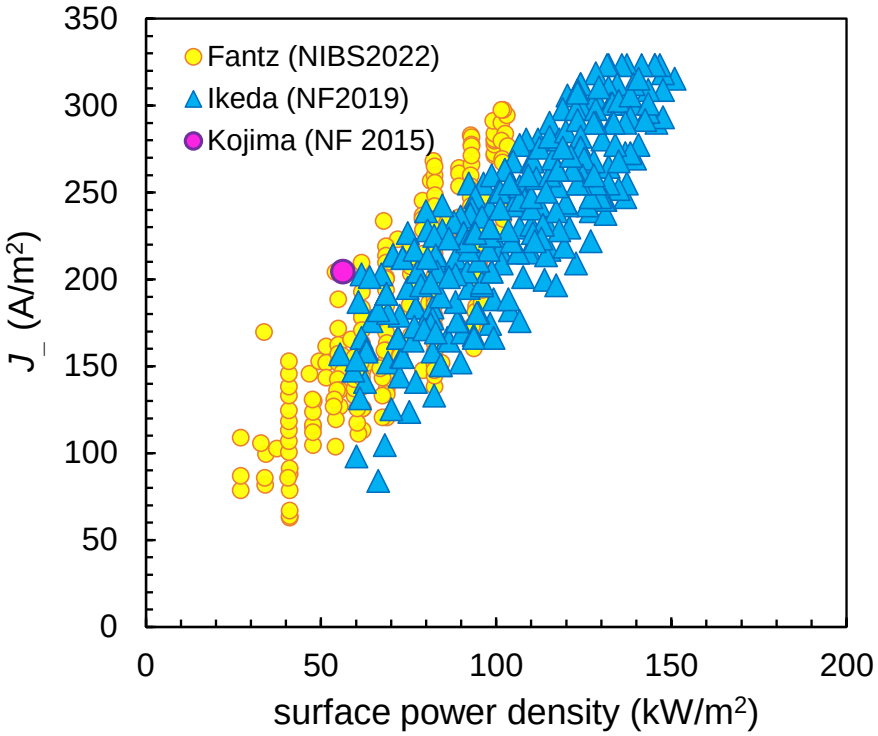

- RF-driven source for ITER to minimize maintenance
- Extracted negative ion current density is comparable

	y	V (m^3)	A(m^2)	B filter	Cs(mg/h)	J_{ext} (A/m^2)	P / P_{plasma}(kW)	I_ (A)	n_H/n_{H2}	α_n	H- divergence @ 25-45kV
LHD H^-source	1998	0.11	1.23	Perm. Magn.	5-7	368	400 / ~360	77	~35%@80kW	~0.7	5.5
JT60SA H^- source	1996	0.41	3.2	Perm. Magn.	12	210	200 / ~180	34			8
1:1 source SPIDER	2018	0.44	5.2	Plasma Grid curr	4-6	200	400 / ~140		~15%@50kW	~1	12
½ source ELISE	2013	0.24	2.9	+ Perm. Magn.	2	303	300 / ~120	30			

Giant negative ion sources

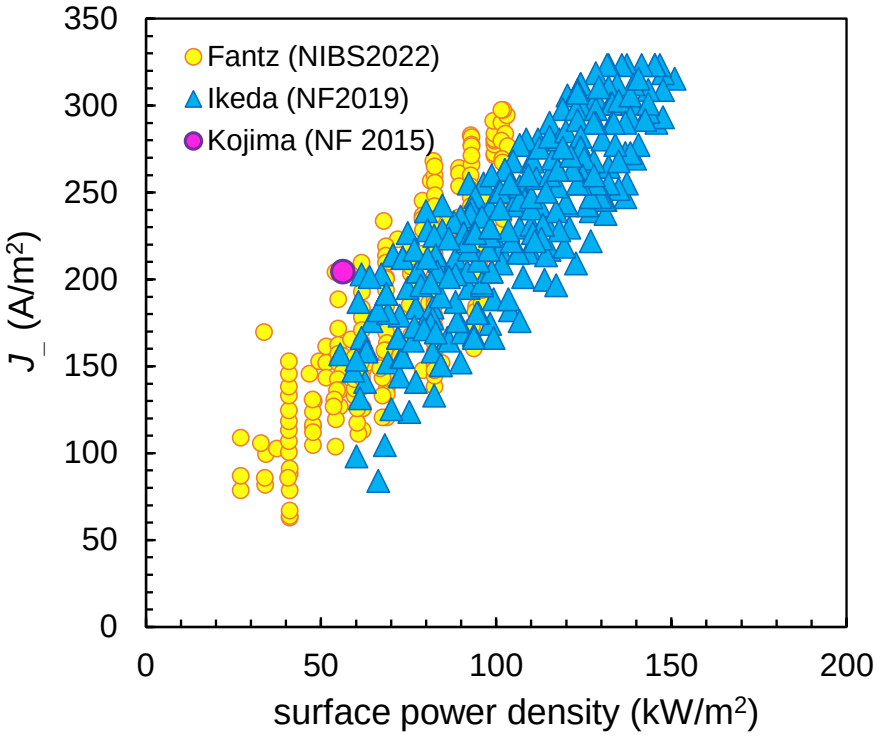

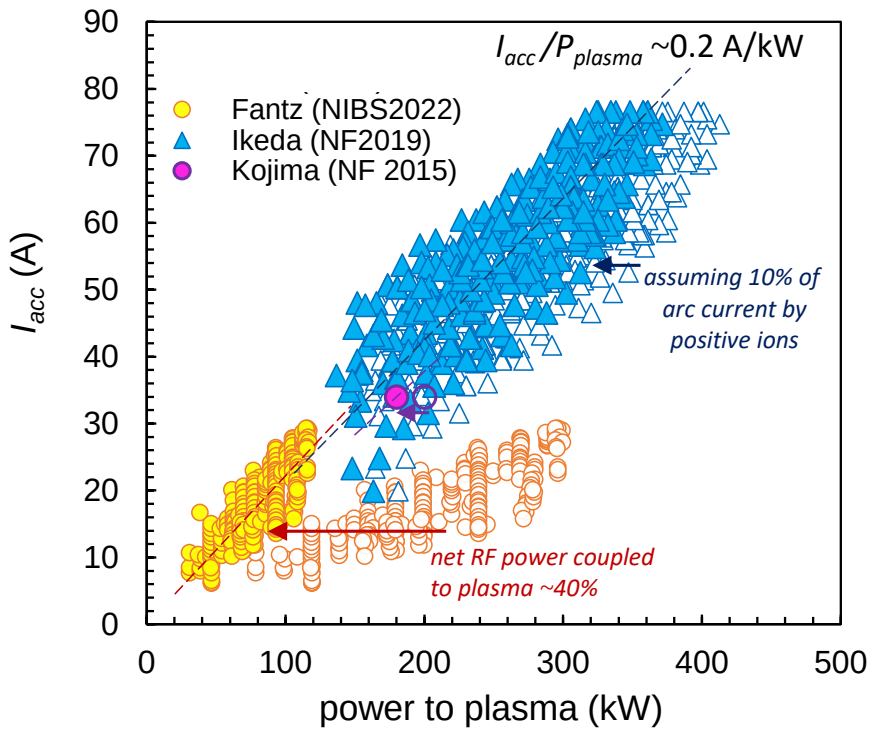

- RF-driven source for ITER to minimize maintenance
- Extracted negative ion current density is comparable
- Considering the effective power coupled to the plasma, the negative ion current scales similarily, despite the different source type

	y	V (m³)	A(m²)	B filter	Cs(mg/h)	J_{ext} (A/m²)	P / P_{plasma}(kW)	I_ (A)	n_H/n_{H2}	α_n	H- divergence @ 25-45kV
LHD H⁻-source	1998	0.11	1.23	Perm. Magn.	5-7	368	400 / ~360	77	~35%@80kW	~0.7	5.5
JT60SA H⁻ source	1996	0.41	3.2	Perm. Magn.	12	210	200 / ~180	34			8
1:1 source SPIDER	2018	0.44	5.2	Plasma Grid curr	4-6	200	400 / ~140		~15%@50kW	~1	12
½ source ELISE	2013	0.24	2.9	+ Perm. Magn.	2	303	300 / ~120	30			

Giant negative ion sources for fusion

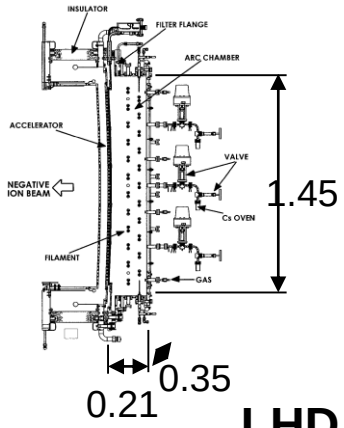

LHD H⁻ source

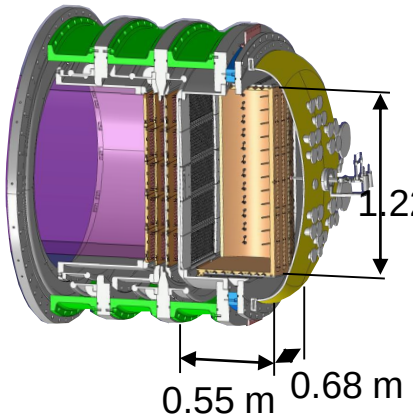

JT60SA H⁻ source

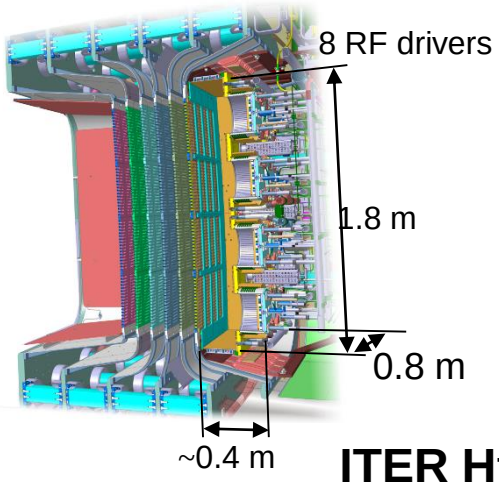

ITER H⁻⁻ source

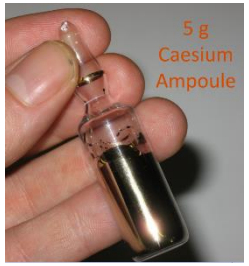

[D. Faircloth, CERN Accelerator School]

Use of caesium to produce neative ions: given the quite short λ_ of negative ions before extraction, **uniform H⁻ production yield** at the extraction region is needed

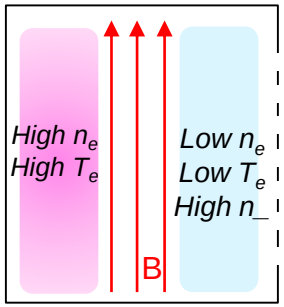

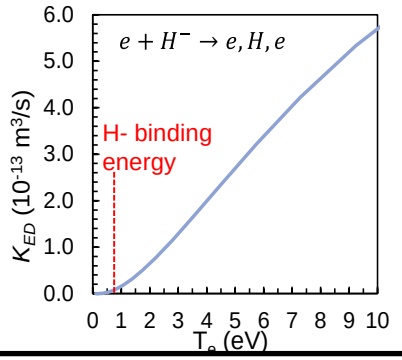

needs **filter field of uniform effectiveness** Difficult design, given large dimensions.
At T_e=2 eV, electron detachment is 3 times faster than at T_e=1 eV

	y	V (m³)	A(m²)	B filter	Cs(mg/h)	J_{ext} (A/m²)	P / P_{plasma}(kW)	I_ (A)	n_H/n_{H2}	α_n	H- divergence @ 25-45kV
LHD H⁻⁻source	1998	0.11	1.23	Perm. Magn.	5-7	368	400 / ~360	77	~35%@80kW	~0.7	5.5
JT60SA H⁻ source	1996	0.41	3.2	Perm. Magn.	12	210	200 / ~180	34			8
1:1 source SPIDER	2018	0.44	5.2	Plasma Grid curr	4-6	200	400 / ~140		~15%@50kW	~1	12
½ source ELISE	2013	0.24	2.9	+ Perm. Magn.	2	303	300 / ~120	30			

Giant negative ion sources for fusion

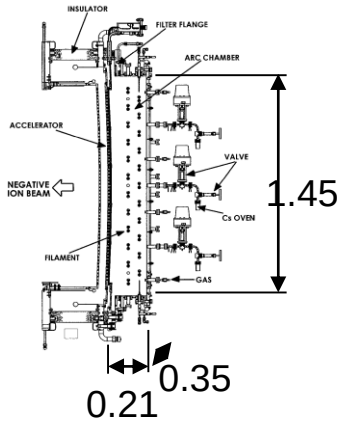

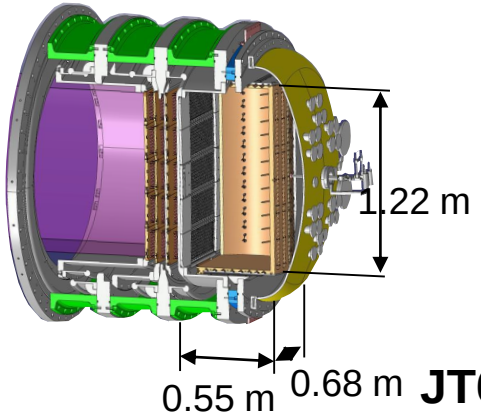

JT60SA H⁻ source

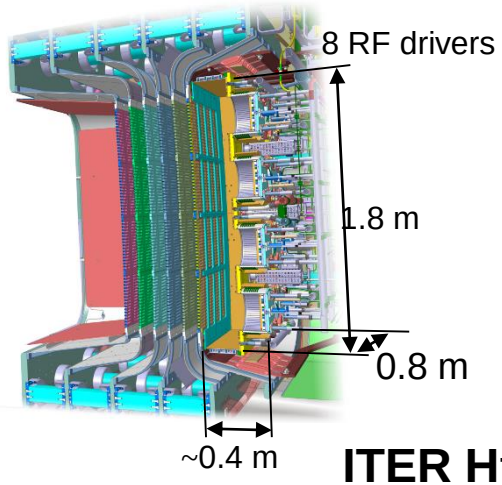

ITER H⁻⁻ source

LHD H⁻ source

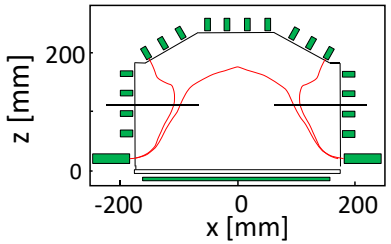

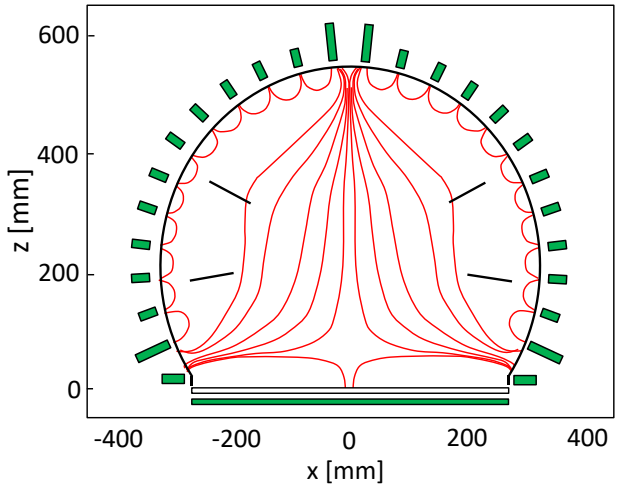

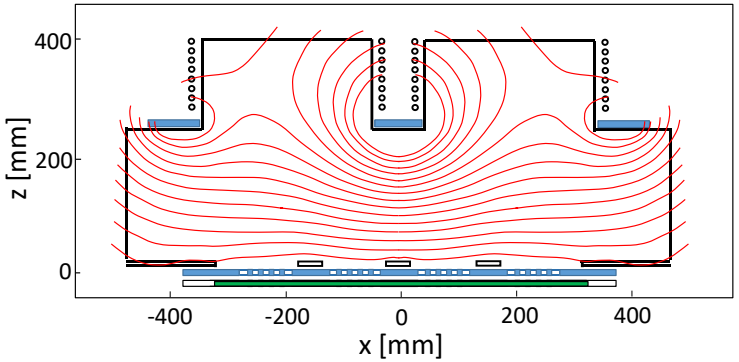

B field used in negative ion sources to separate in two regions the plasma: tandem concept implies vertical drifts (magnetised electrons)

$$v_{\nabla B}^{drift} = (mv_{\perp}^2/2qB)\,\boldsymbol{B} \times \nabla B/B^2$$

$$v_{E\times B}^{drift} = \boldsymbol{E} \times \boldsymbol{B}/B^2$$

$$v_{\nabla p\times B}^{drift} = -\nabla p_e \times \boldsymbol{B}/B^2$$

on electrons, dominant term in the bulk plasma, if potential is uniform

Giant negative ion sources for fusion

LHD H^- source

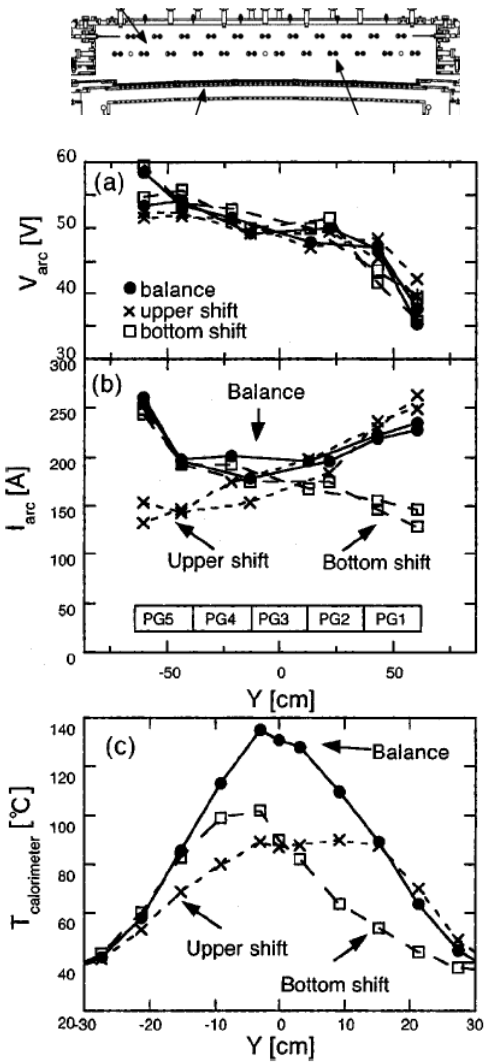

JT60SA H^- source

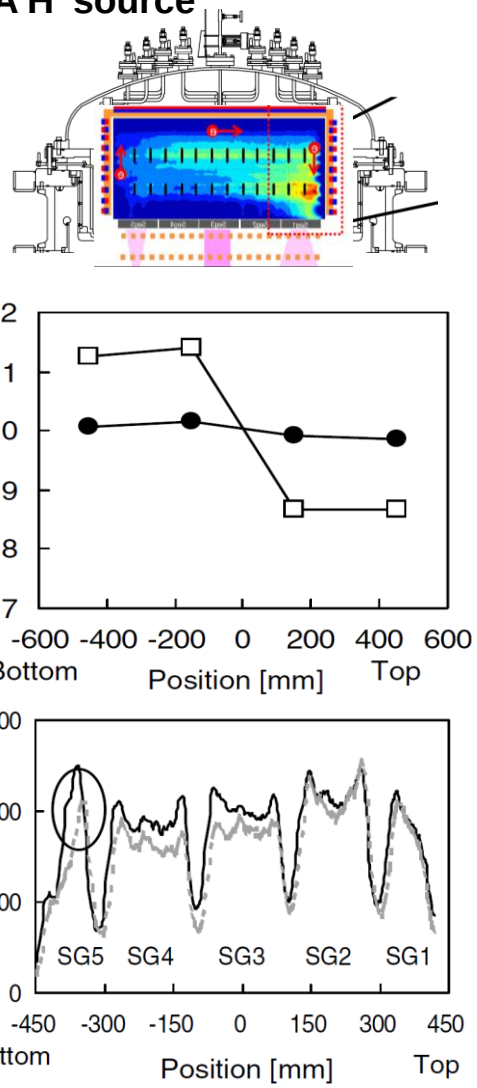

SPIDER

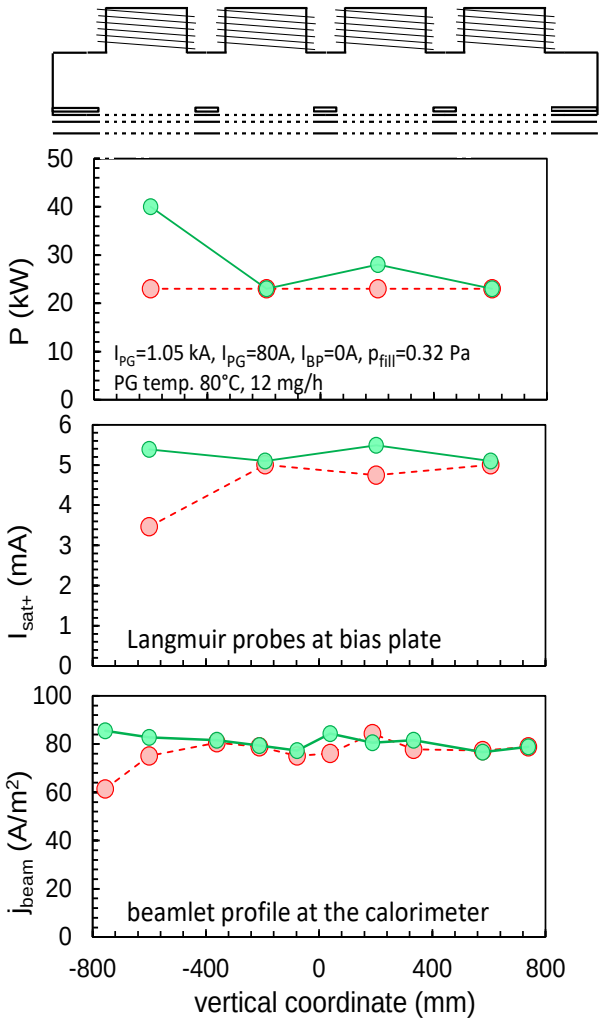

Common to giant sources:

Plasma drifts perpendicular to filter field cause non-homogeneities of extracted current

May be counterbalanced by modulating the discharge power along the vertical direction (filaments or RF drivers)

Magnetic configurations that compensate the vertical drifts may not be applicable to all source types…

And non-homogeneity may be specific of one type

Umeda Nucl. Fusion **43** (2003) 522–526
Ikeda Rev. Sci. Instrum., Vol. 75, No. 5, May 2004
Kojima Nucl. Fusion **55** (2015) 063006
S. Fujita,et al. AIP Conf Proc **1869**, 030041 (2017)

Giant negative ion sources for fusion

ELISE

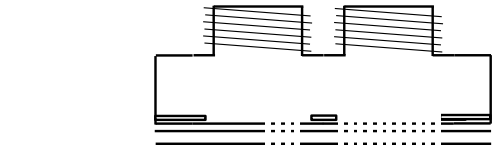

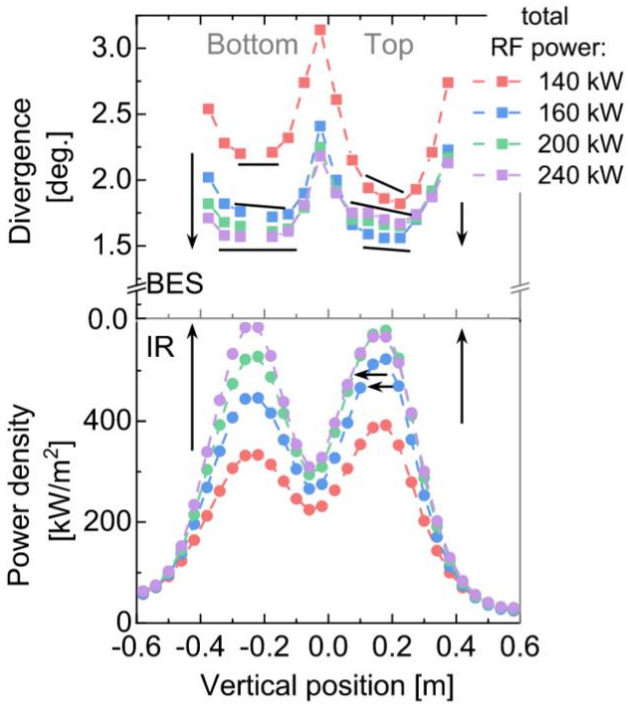

Uext = 6 kV, Uacc = 30 kV and IPG = 3.7 kA

SPIDER

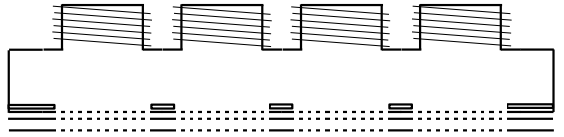

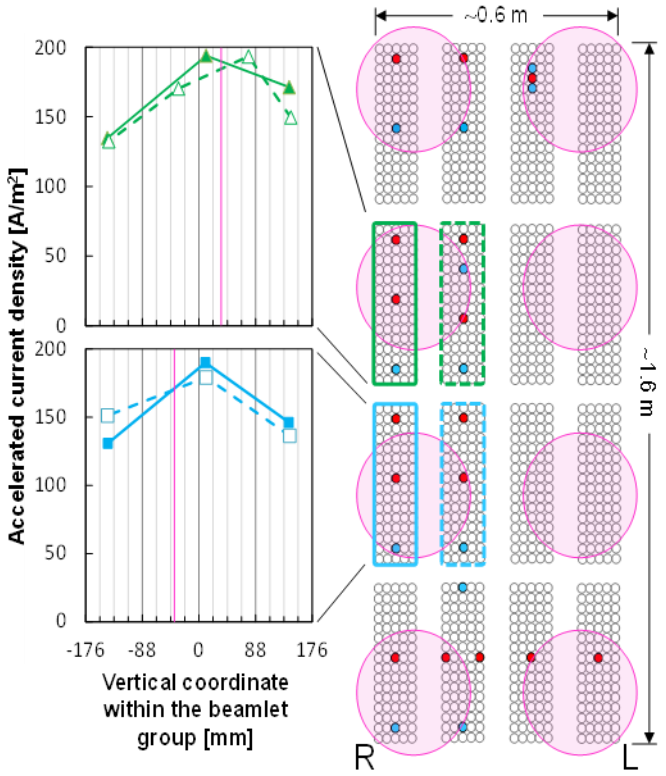

P_{RF}=4×100 kW, U_{ex}=8.5 kV, U_{acc}=39.5 kV, $j_e/j_- \approx 0.4$ *w/ caesium*

Common to giant sources:

Plasma drifts perpendicular to filter field cause non-homogeneities of extracted current

May be counterbalanced by modulating the discharge power along the vertical direction (filaments or RF drivers)

Magnetic configurations that compensate the vertical drifts may not be applicable to all source types…

And non-homogeneity may be specific of one type

Mario Nucl. Fusion 60 (2020) 066025
Sartori Fus Eng Des194, 113730 (2023)

Giant negative ion sources

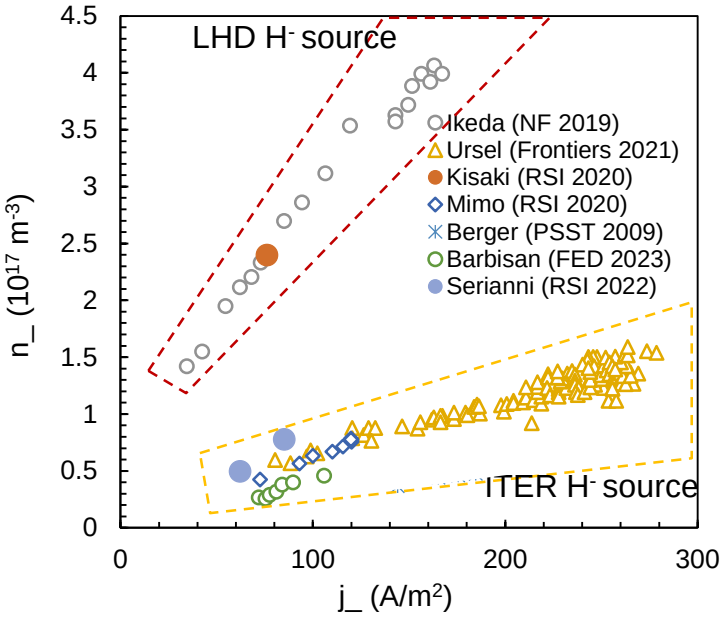

[1] Serianni RSI
[2] Tsumori
[3] Fujiwara
[4] Pimazzoni

- Different proportionality term $j_- \propto n_-$

$$j_- = eh\left(\frac{k_B T_+}{m_-}\right)^{1/2} \cdot n_-$$ Direct influence of positive ions

$$j_- = e\frac{1}{4}\left(\frac{8k_B T_-}{\pi m_-}\right)^{1/2} \cdot n_-$$ influence of positive ions via Coulomb collisions

- Depending on the value of *h*, an effective T_+ between 0.6 and 1.6 eV was extrapolated for SPIDER [1]

	y	V (m^3)	A(m^2)	B filter	Cs(mg/h)	J_{ext} (A/m^2)	P / P_{plasma}(kW)	I_- (A)	n_H/n_{H2}	α_{-}	H- divergence @ 25-45kV
LHD H⁻-source	1998	0.11	1.23	Perm. Magn.	5-7	368	400 / ~360	77	~35%@80kW	~0.7	5.5
JT60SA H⁻ source	1996	0.41	3.2	Perm. Magn.	12	210	200 / ~180	34			8
1:1 source SPIDER	2018	0.44	5.2	Plasma Grid curr	4-6	200	400 / ~140		~15%@50kW	~1	12
½ source ELISE	2013	0.24	2.9	+ Perm. Magn.	2	303	300 / ~120	30			

Giant negative ion sources

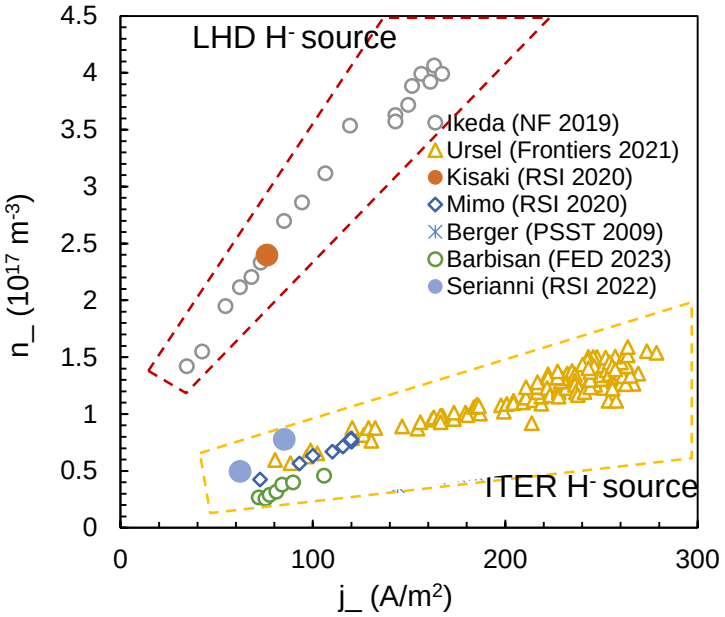

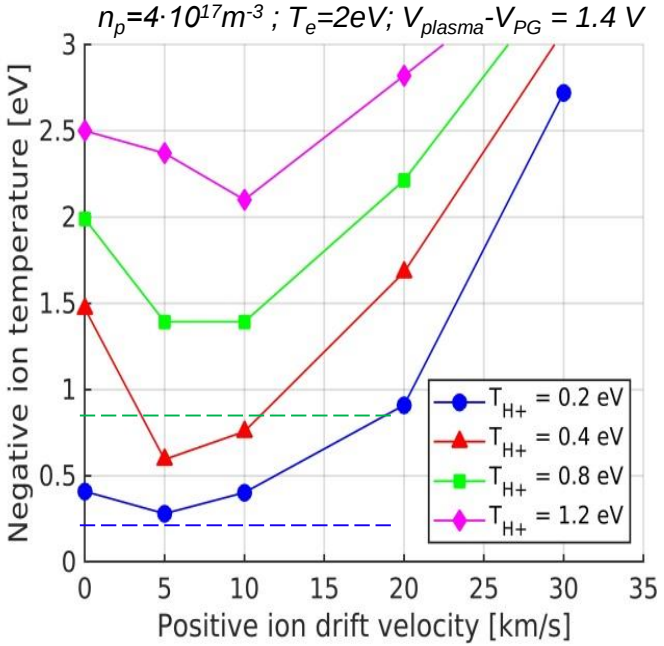

[1] Serianni RSI
[2] Tsumori
[3] Fujiwara
[4] Pimazzoni

- Different proportionality term $j_- \propto n_-$

$$j_- = eh\left(\frac{k_B T_+}{m_-}\right)^{1/2} \cdot n_-$$ Direct influence of positive ions

$$j_- = e\frac{1}{4}\left(\frac{8k_B T_-}{\pi m_-}\right)^{1/2} \cdot n_-$$ influence of positive ions via Coulomb collisions

- Depending on the value of *h*, an effective T_+ between 0.6 and 1.6 eV was extrapolated for SPIDER [1]
- It is well known that multicusp arc chambers have low ion temperature. In filament art source T_ is measured of the order of 0.1-0.3 eV. [2]
- Velocity of negative ions at meniscus as a cause of divergence, hence reduced beam efficiency [3,4]

	y	V (m^3)	A(m^2)	B filter	Cs(mg/h)	J_{ext} (A/m^2)	P / P_{plasma}(kW)	I_- (A)	n_H/n_{H2}	α_{-}	H- divergence @ 25-45kV
LHD H⁻source	1998	0.11	1.23	Perm. Magn.	5-7	368	400 / ~360	77	~35%@80kW	~0.7	5.5
JT60SA H⁻ source	1996	0.41	3.2	Perm. Magn.	12	210	200 / ~180	34			8
1:1 source SPIDER	2018	0.44	5.2	Plasma Grid curr	4-6	200	400 / ~140		~15%@50kW	~1	12
½ source ELISE	2013	0.24	2.9	+ Perm. Magn.	2	303	300 / ~120	30			

Giant negative ion sources

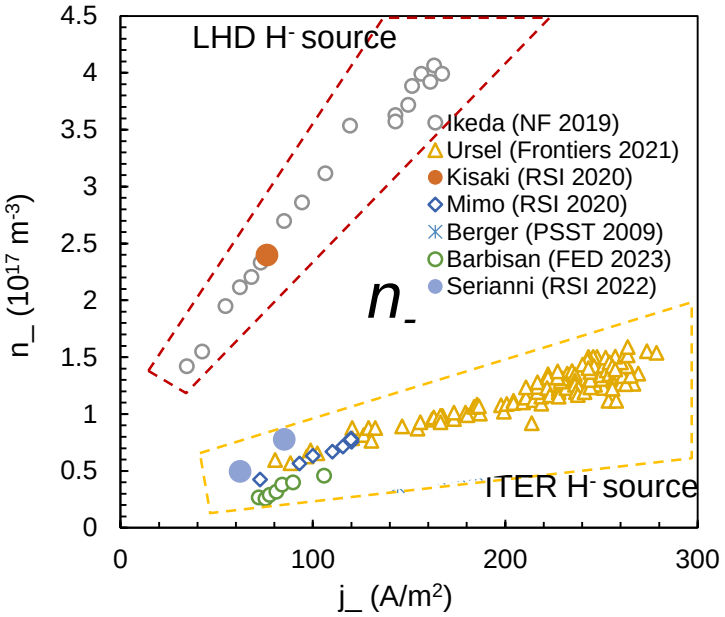

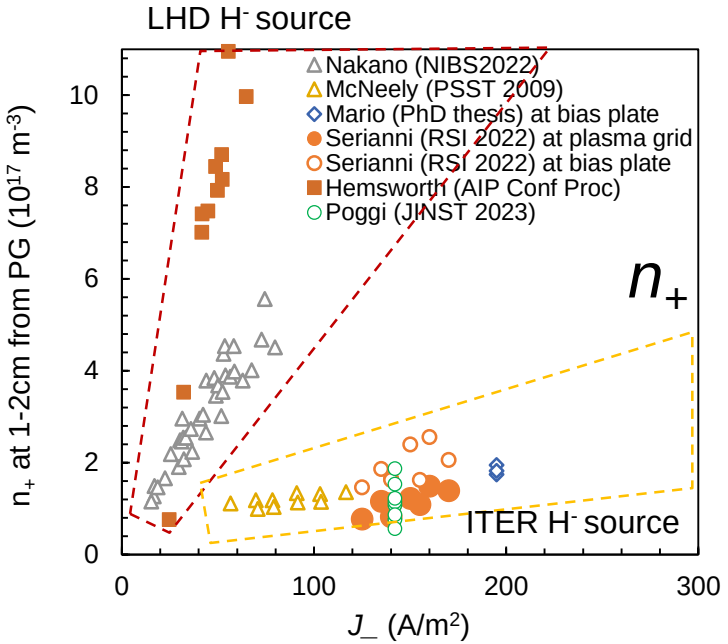

- Different properties at the extraction region
- The proportion are more or less similar: elettronegativity $\alpha_- = n_-/n_e$ appears similar (between 0.7 and 1): negative ion density not limited by the negative ion production

	y	V (m^3)	A(m^2)	B filter	Cs(mg/h)	J_{ext} (A/m^2)	P / P_{plasma}(kW)	I_ (A)	n_H/n_{H2}	α_-	H- divergence @ 25-45kV
LHD H⁻-source	1998	0.11	1.23	Perm. Magn.	5-7	368	400 / ~360	77	~35%@80kW	~0.7	5.5
JT60SA H⁻ source	1996	0.41	3.2	Perm. Magn.	12	210	200 / ~180	34			8
1:1 source SPIDER	2018	0.44	5.2	Plasma Grid curr	4-6	200	400 / ~140		~15%@50kW	~1	12
½ source ELISE	2013	0.24	2.9	+ Perm. Magn.	2	303	300 / ~120	30			

Motivations of this work and Outline

There are **common features** but also **fundamental differences** between the ion sources for fusion.
If the accelerator is optimized, fundamental features in the beam and non-homogeneties can traced back to the plasma.

The plasma properties at the extraction region highlight differences: depend on **plasma formation** and plasma **transport through the filter field** from the driver

Understanding driver and expansion regions of the source is key to **reach the targets of the ITER H- source**.

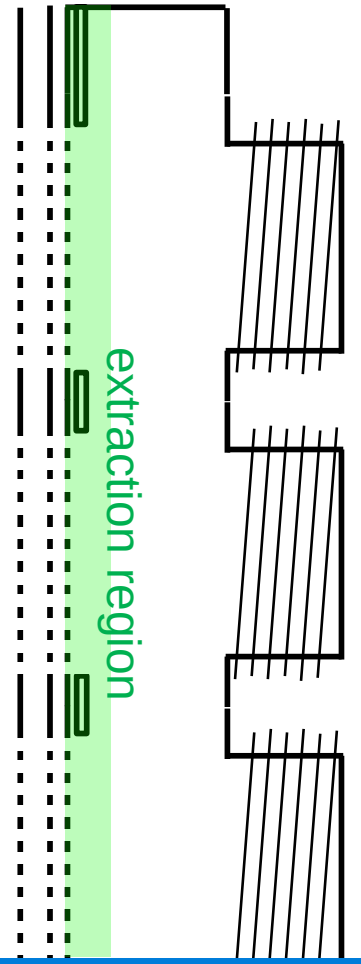

SUMMARY OF RESULTS

- plasma parameters at the extraction region of SPIDER
- plasma parameters along expansion region in SPIDER
- plasma parameters inside RF drivers in SPIDER
- positive ion energy distribution in fiament arc and RF-driven sources

Plasma uniformity at extraction apertures

- (Almost) all SPIDER diagnostics used for this analysis
- Purpose: study the role of caesium in negative ion production and beam uniformity
- H_2 discharge 50 kW, repeated with higher caesium injection

Source diagnostics
Electrical currents
Calorimetry and surface thermocouples
Electrostatic probes
Source optical emission spectroscopy (OES)
Cavity ring down spectroscopy (CRDS)
Laser absorption spectroscopy (LAS)
Beam diagnostics
Calorimetry and surface thermocouples
Beamlet current monitors
Instrumented calorimeter STRIKE
Allison emittance scanner
Beam emission spectroscopy (BES)
Optical tomography
Neutron imaging

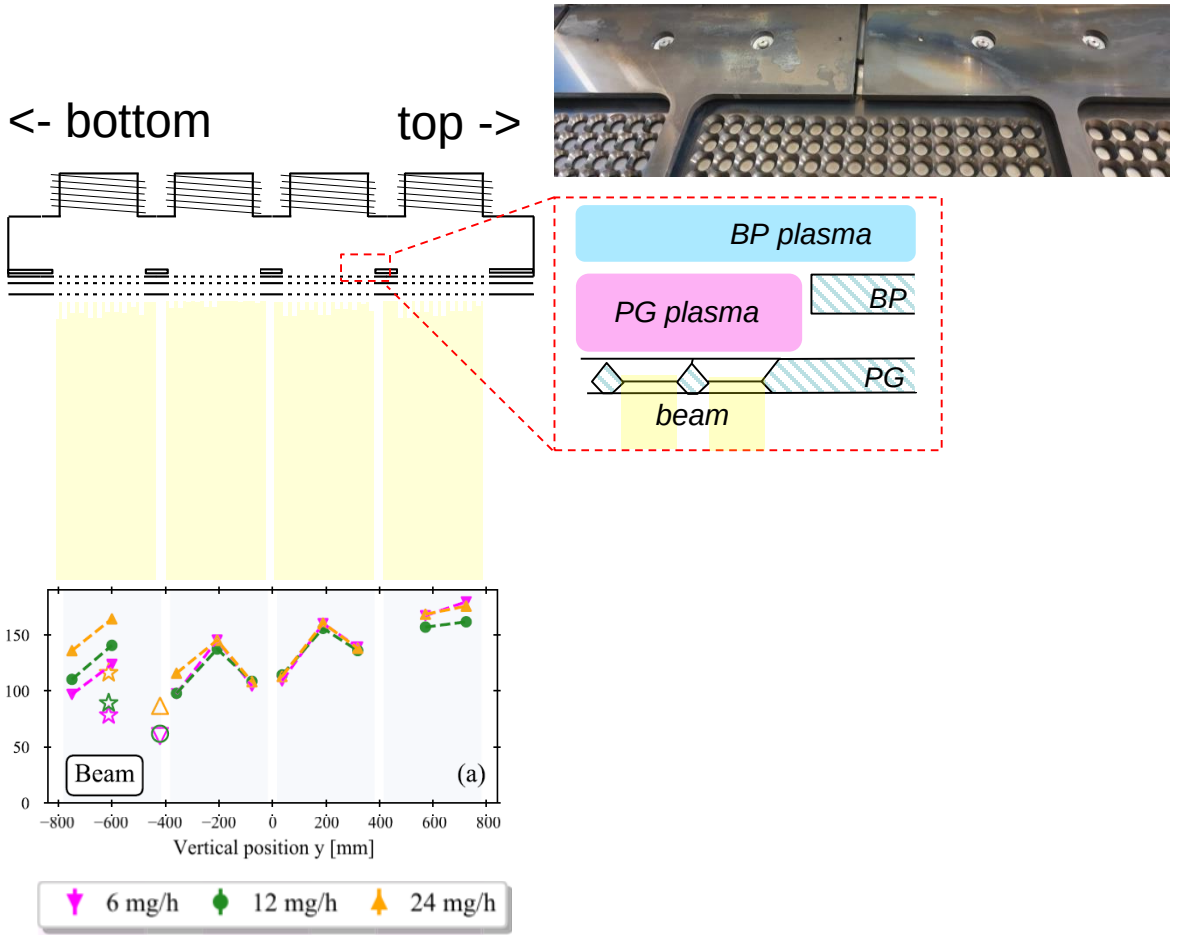

Plasma uniformity at extraction apertures

- (Almost) all SPIDER diagnostics used for this analysis
- Purpose: study the role of caesium in negative ion production and beam uniformity
- H_2 discharge 50 kW

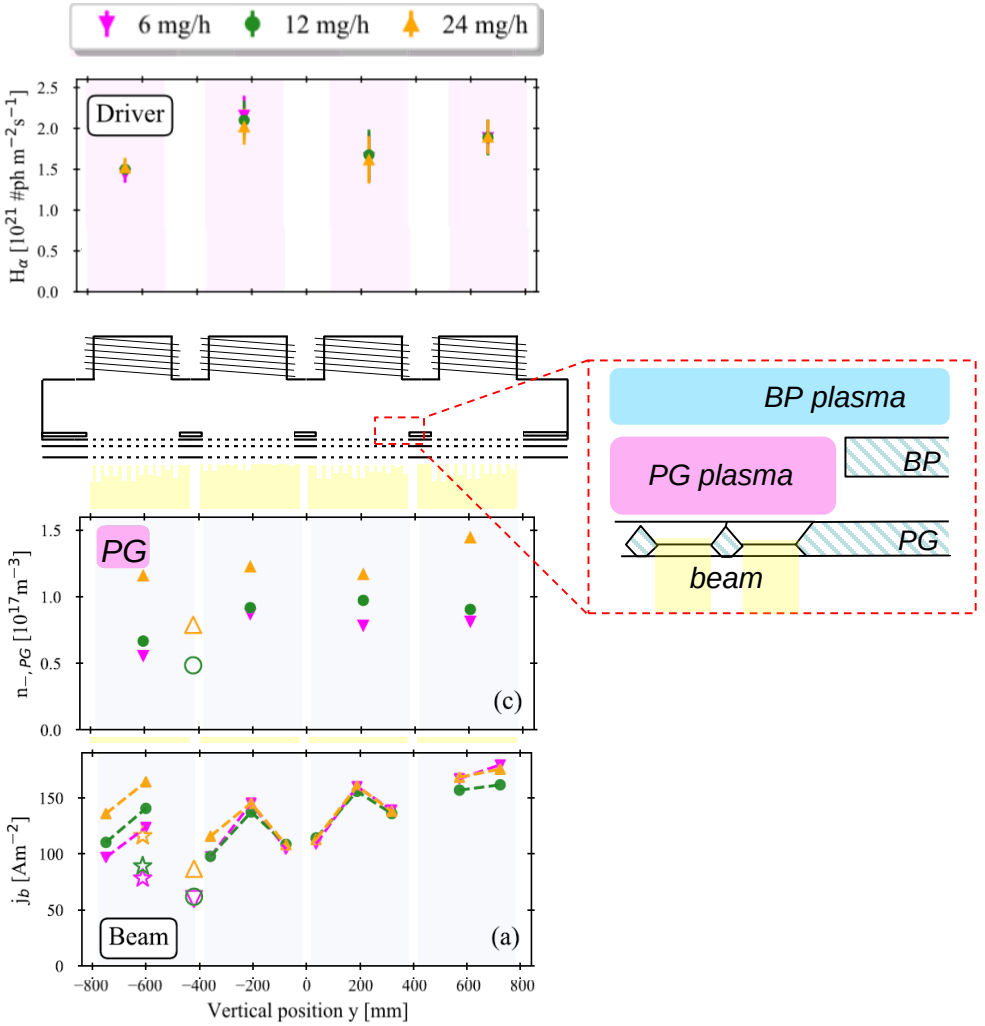

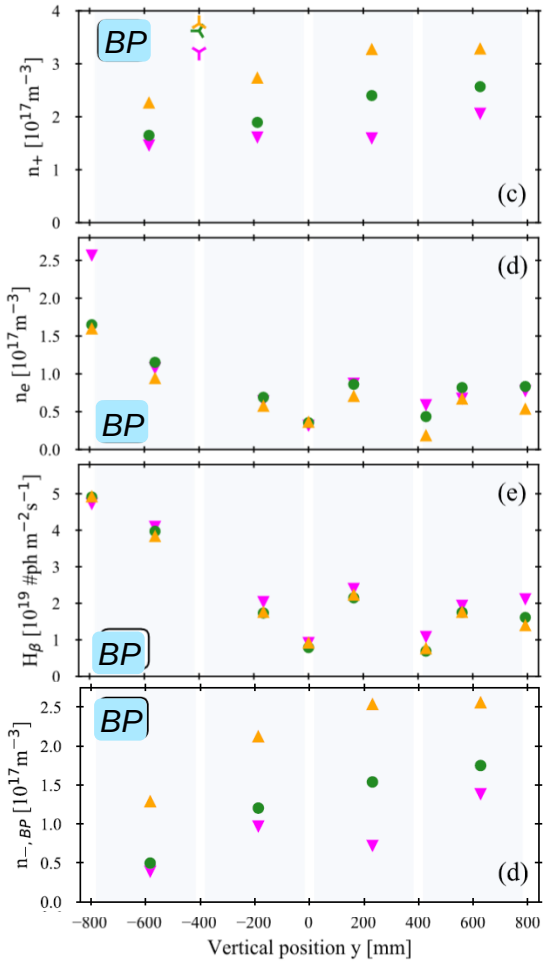

Plasma uniformity at extraction apertures

- (Almost) all SPIDER diagnostics used for this analysis
- Purpose: study the role of caesium in negative ion production and beam uniformity
- H_2 discharge 50 kW.
- At the bottom, less positive ions; less beamlet current; caesium evaporation improves both.
- Plasma parameters inside drivers appear to be uneven (also left right have different behaviours)
- Electron drift downwards

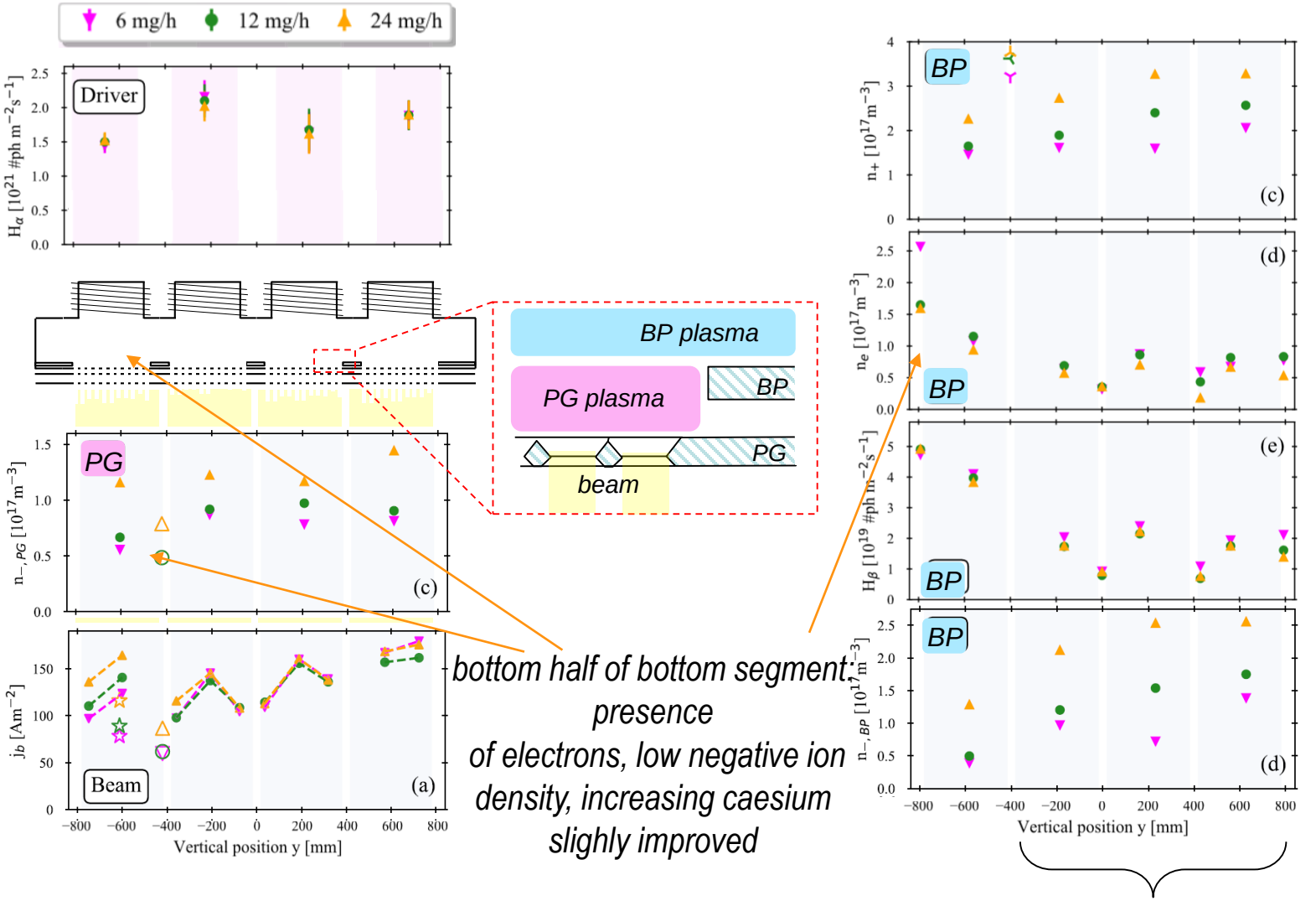

Serianni, et al., Rev. Sci. Instrum. **93**, 081101 (2022); doi: 10.1063/5.0084797

OUTLINE

- plasma parameters at the extraction region of SPIDER
- plasma parameters along expansion and driver regions in SPIDER
- positive ion energy distribution in fiament arc and RF-driven sources

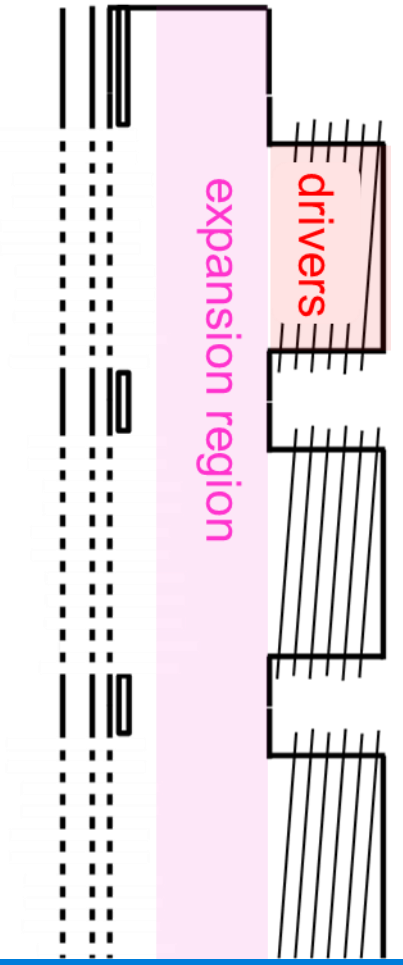

Axial profiles of plasma parameters

- temporary movable system in vacuum used to enter the ion source from the accelerator (no beam ☺)
- multiple probes to enter at different positions; effect of filter field, pressure, bias, position, RF power was investigated
- magnetic field on the horizontal section

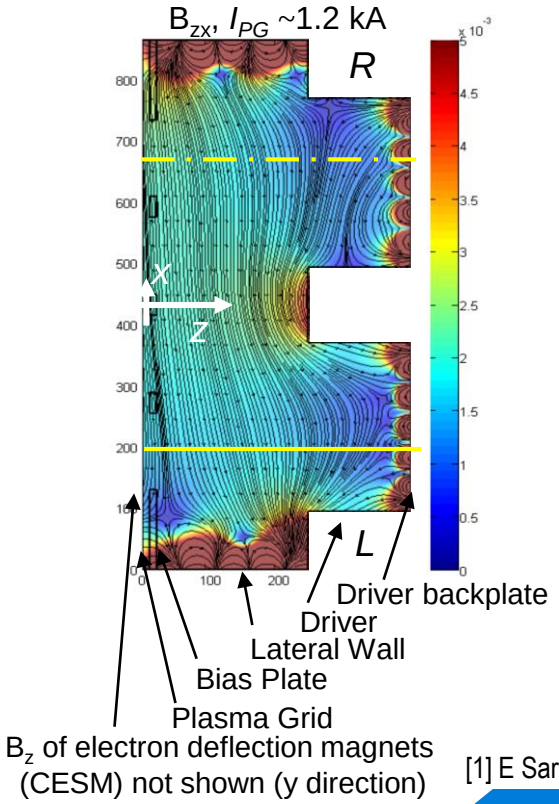

[1] E Sartori, et al., Fus Eng Des 169, 112424 (2021)

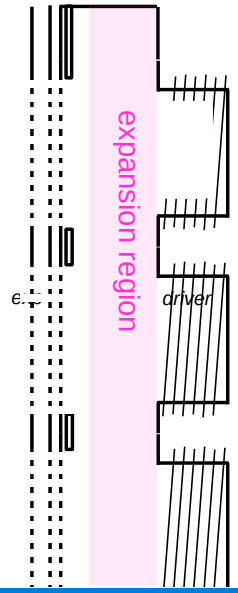

Axial profiles of plasma parameters

- temporary movable system in vacuum used to enter the ion source from the accelerator (no beam ☺)
- multiple probes to enter at different positions; effect of filter field, pressure, bias, position, RF power was investigated
- magnetic field on the horizontal section

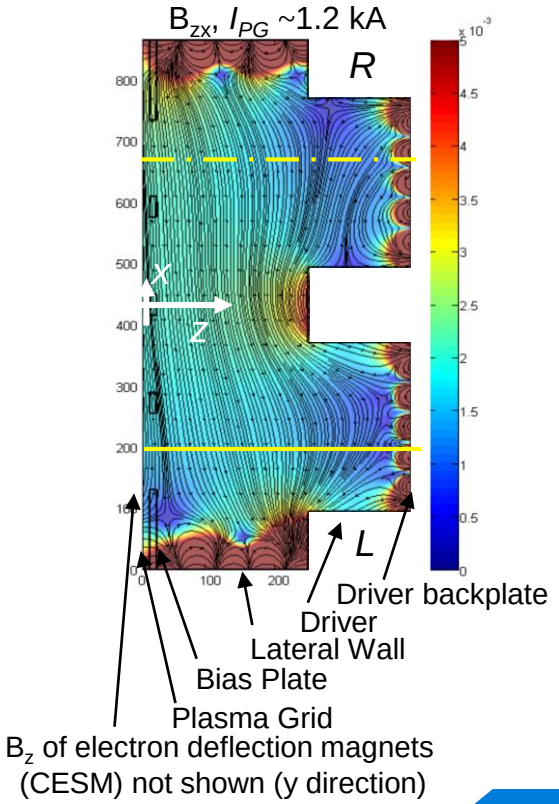

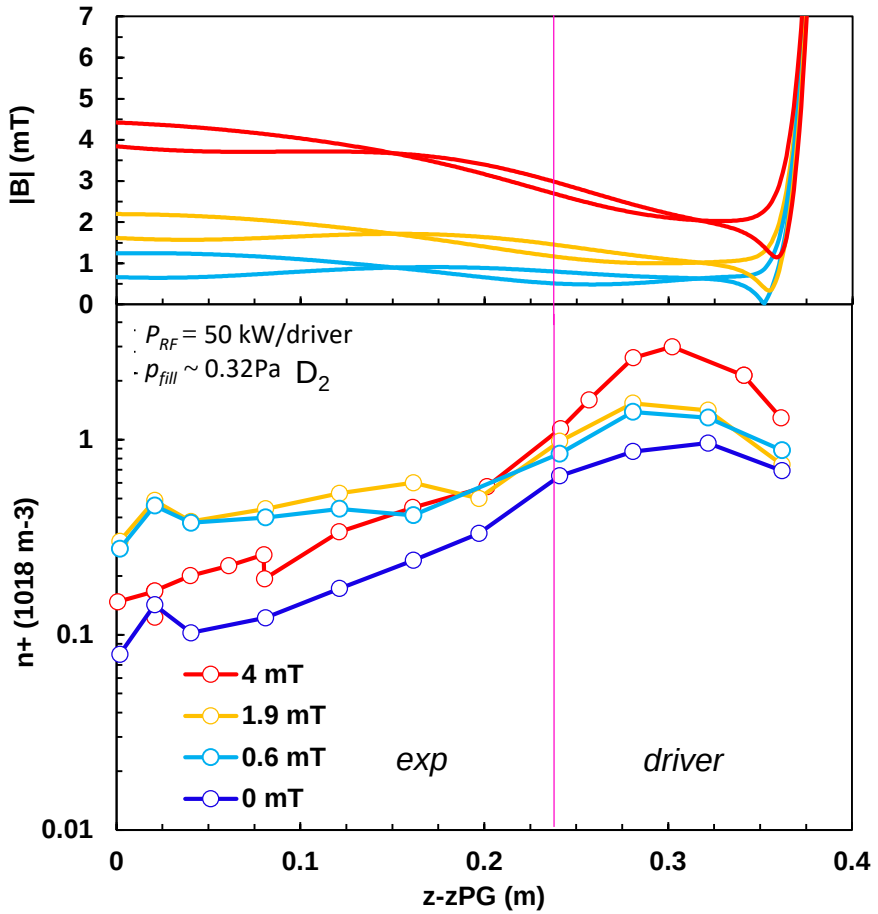

- Perpendicular filter field limits plasma diffusion: plasma density confined inside driver (up to a threshold)
- Expansion: diffusion through a perpendicular field, no ionization, rather uniform $D_{a,\perp}$: as expected linear decrease of plasma density

Axial profiles of plasma parameters

- temporary movable system in vacuum used to enter the ion source from the accelerator (no beam ☺)
- multiple probes to enter at different positions; effect of filter field, pressure, bias, position, RF power was investigated
- magnetic field on the horizontal section

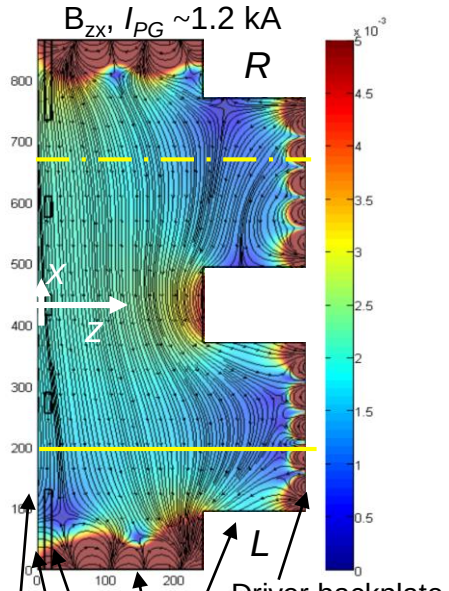

B_z of electron deflection magnets (CESM) not shown (y direction)

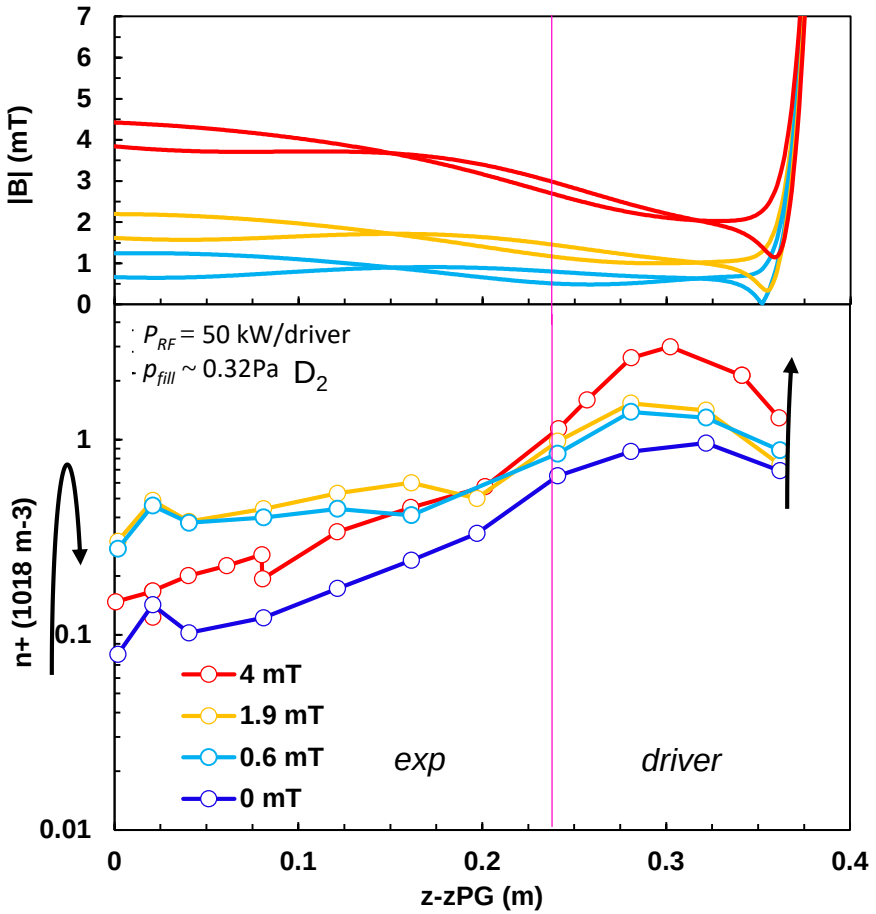

- Perpendicular filter field limits plasma diffusion: plasma density confined inside driver (up to a threshold)
- Expansion: diffusion through a perpendicular field, no ionization, rather uniform $D_{a,\perp}$: as expected linear decrease of plasma density

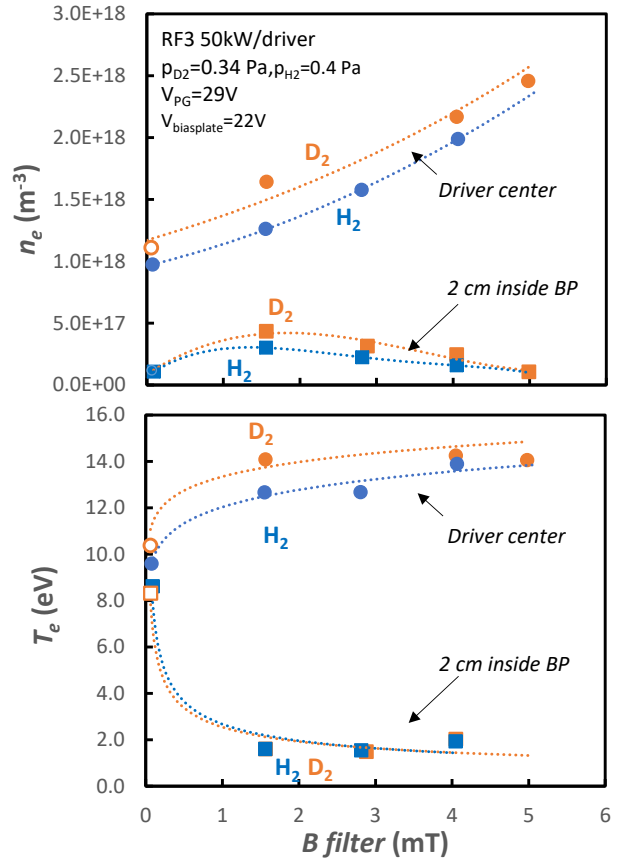

Perpendicular filter field limits plasma diffusion: plasma density confined inside driver (up to a threshold for some drivers). Zero-order solution of the axial diffusion [1] indicates linear dependence on $B_\perp$

$$n_{e,driver} \approx n_{e,exp} + \frac{0.5}{K_{iz} n_{gas}} \cdot \frac{e \nu_{mi}}{\gamma m_e} B_\perp$$

Expansion: diffusion through a perpendicular field, no ionization, rather uniform $D_{a,\perp}$, diminish as $B^2_\perp$

[1] P. Jain, et al., Plasma Phys. Control. Fusion 65 (2023) 095010

Axial profiles of plasma parameters

- temporary movable system in vacuum used to enter the ion source from the accelerator (no beam ☺)
- multiple probes to enter at different positions; effect of filter field, pressure, bias, position, RF power was investigated
- magnetic field on the horizontal section

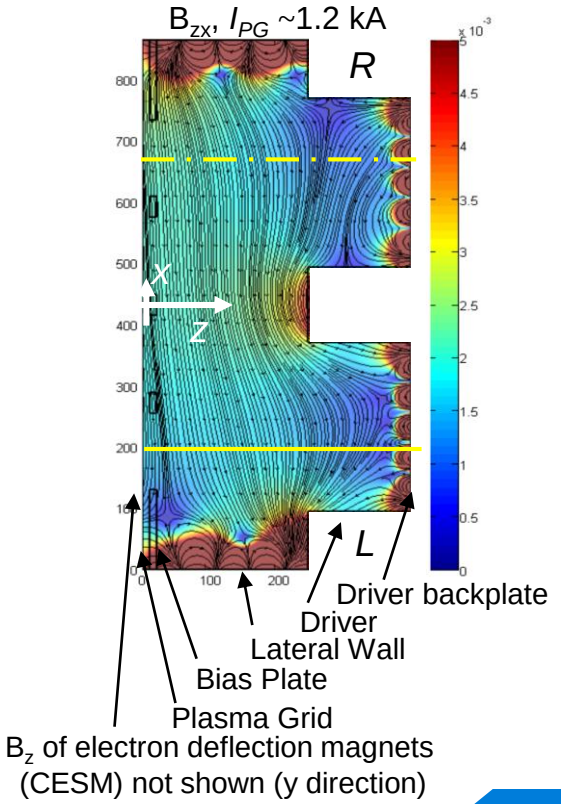

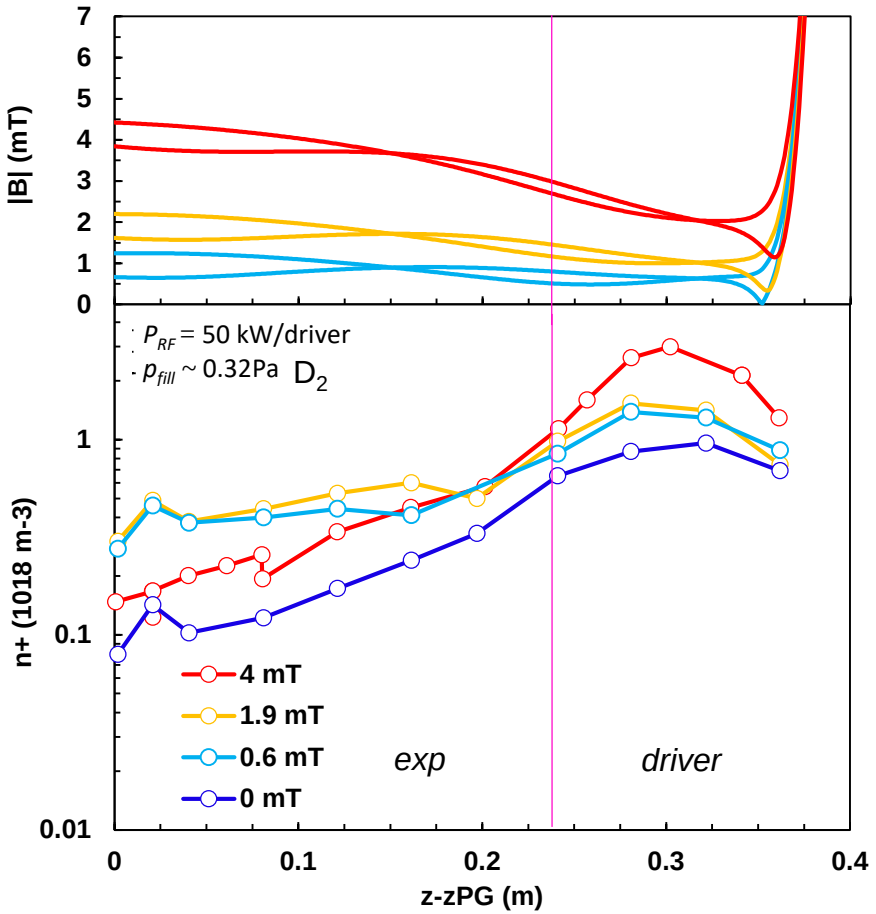

- Perpendicular filter field limits plasma diffusion: plasma density confined inside driver (up to a threshold)
- Expansion: diffusion through a perpendicular field, no ionization, rather uniform $D_{a,\perp}$: as expected linear decrease of plasma density

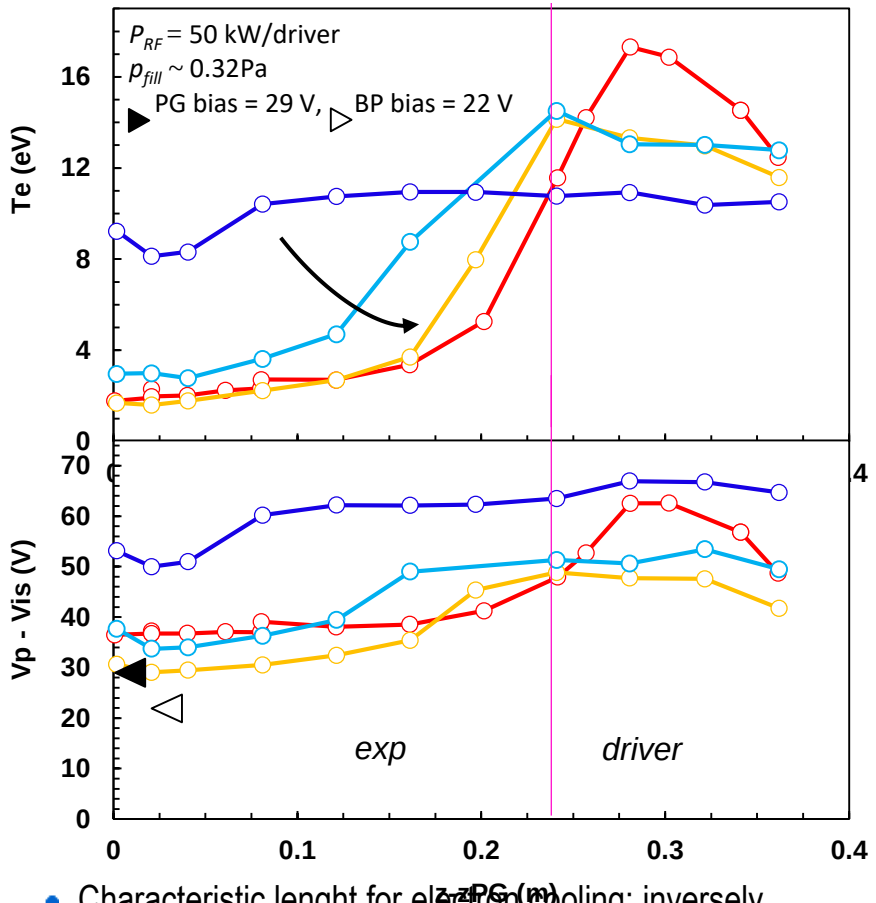

- Characteristic lenght for electron cooling: inversely proportional to $B_\perp$
- Plasma potential wrt ion source walls: Vp-Vis always rather high at ~0.3 Pa
- At extraction region: minimum Vp-VPG at intermediate values of $B_\perp$ ~2 mT, in correspondence of a maximum value of n+, and minimum of Te

Axial profiles of plasma parameters: pressure and bias

- temporary movable system in vacuum used to enter the ion source from the accelerator (no beam ☺)
- multiple probes to enter at different positions; effect of filter field, pressure, bias, position, RF power was investigated
- magnetic field on the horizontal section

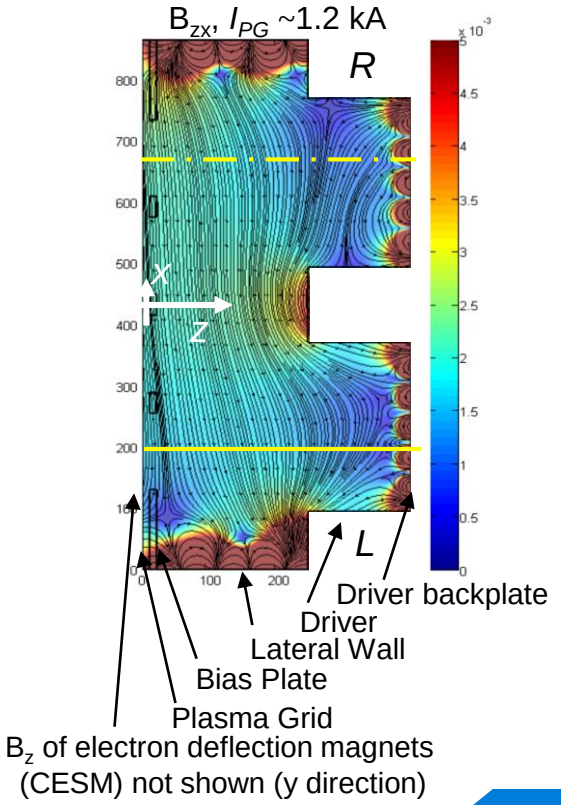

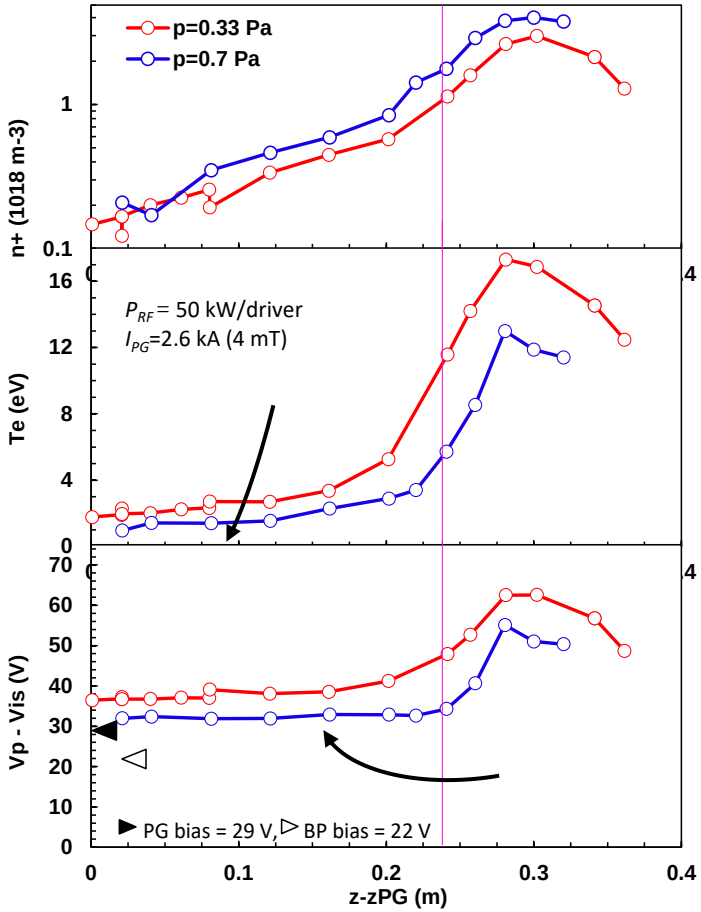

- with higher pressures, Te decreases down to 1 eV at the extraction region, the potential profile get flat
- Along the expansion region, plasma density is low, and collisions against molecule play a role in the perpendicular diffusion and electron cooling

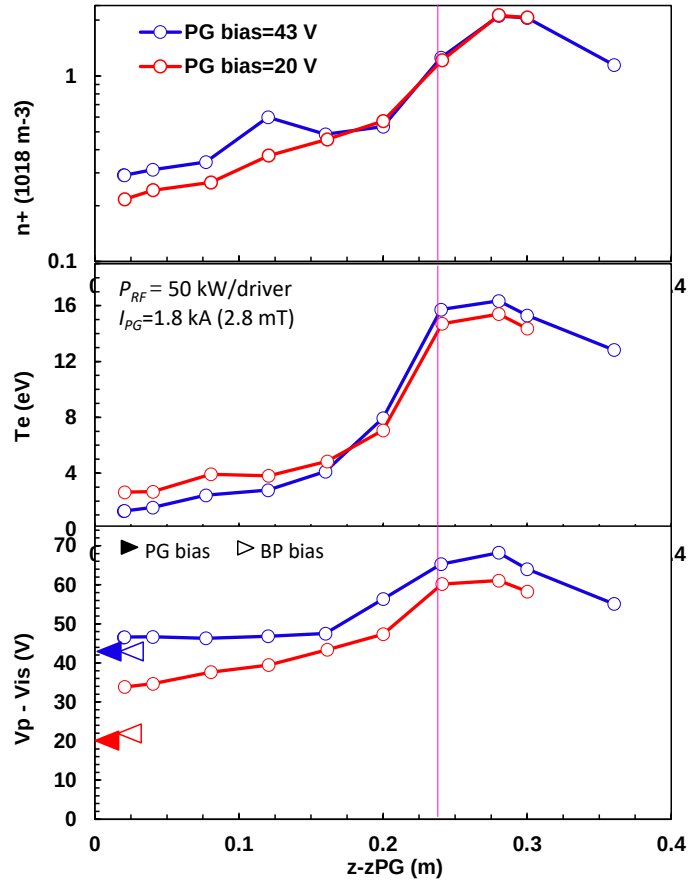

- Also by increasing the bias voltage of the plasma grid, Te decreases down to 1 eV, and the potential profile flattens out

Expansion from drivers

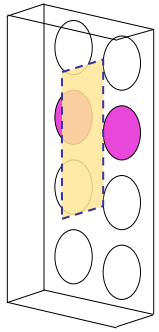

single generator; 2D measurements not exactly on midplane

interpolation of probe measurements

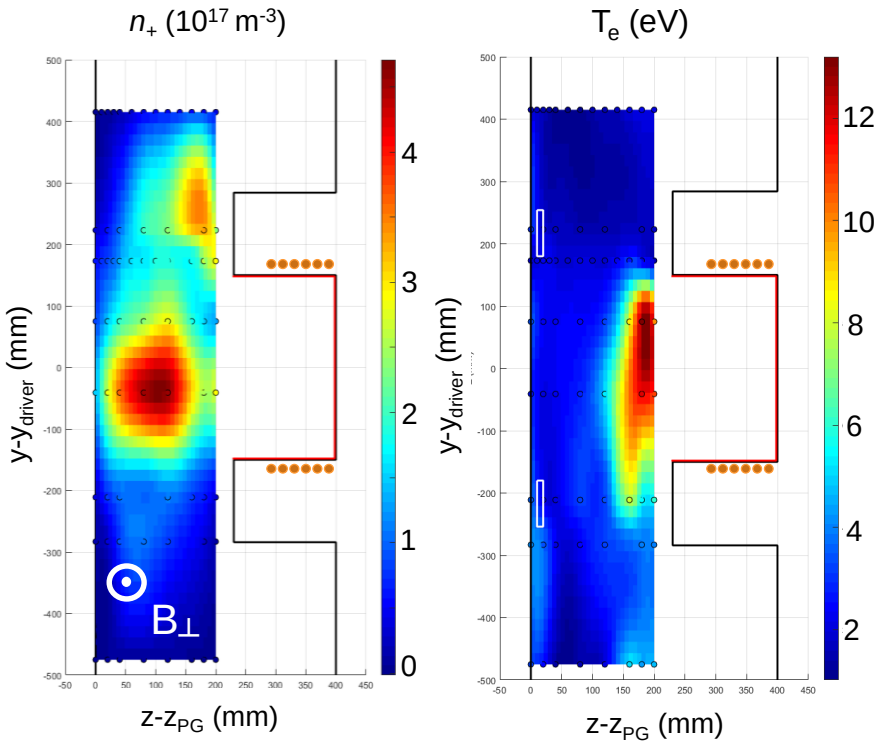

Predicted by modeling

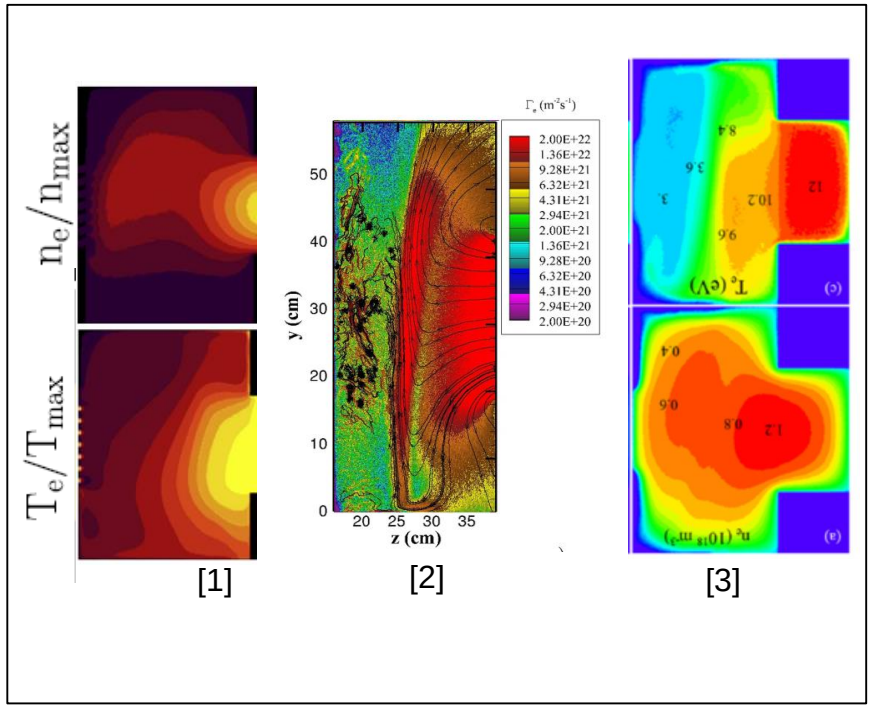

- top/bottom separation of positive and negative charges (ExB)
- hall current of hot electrons leaking from drivers [1,2,3] confirmed experimentally (ExB for electrons same direction as gradP x B)

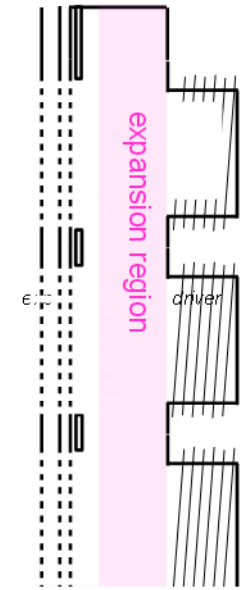

[1] G. Fubiani, et al., New J. Phys. 19 (2017) 015002
[2] F Taccogna and P Minelli, New J. Phys. 19 (2017) 015012
[3] Boeuf et al. Phys. Plasmas 19, 113510 (2012)

Expansion from drivers

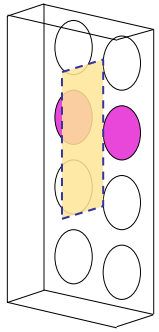

single generator; 2D measurements not exactly on midplane

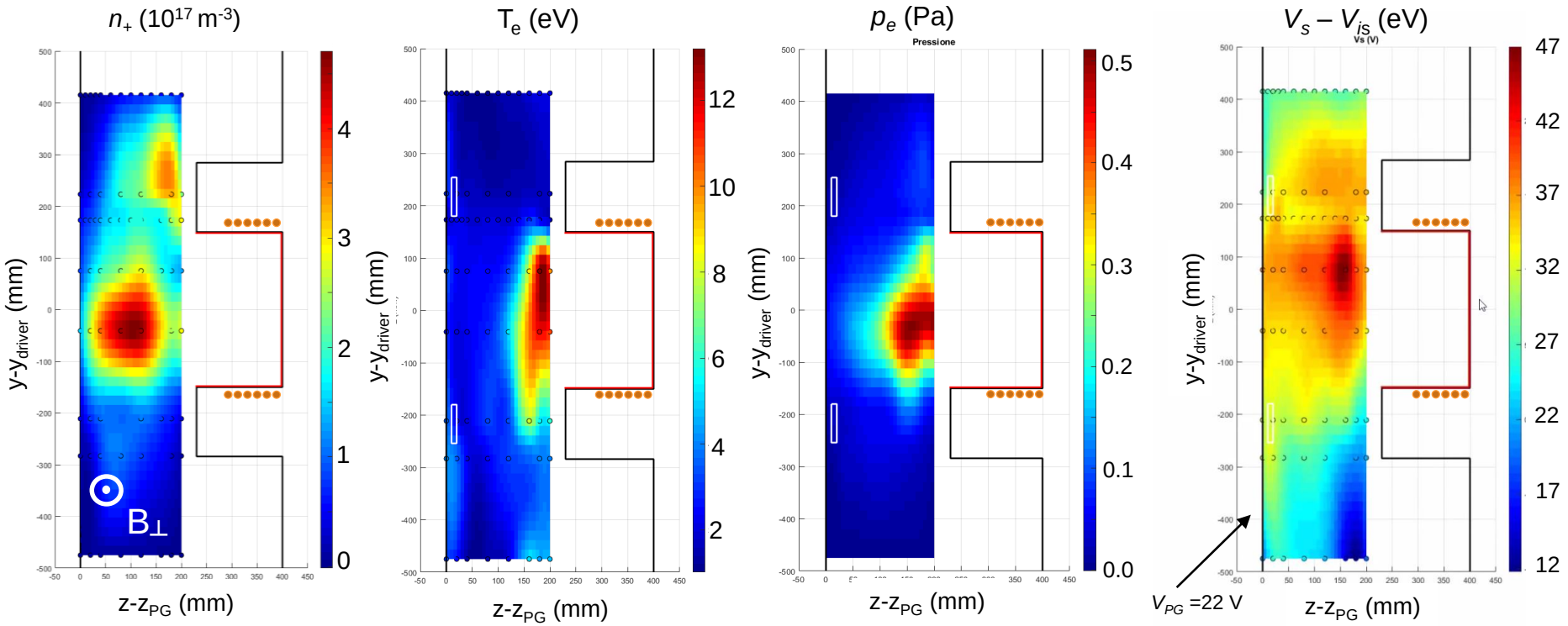

- top/bottom separation of positive and negative charges (ExB)
- hall current of hot electrons leaking from drivers [1,2,3] confirmed experimentally (ExB for electrons same direction as gradP x B)
- quite symmetric top/bottom electron pressure $p_e=n_ekT_e$
- top/bottom non uniformity of plasma potential at the extraction region originates in the expansion region;

Spatial distribution inside drivers: ongoing work

- Plasma inside RF Driver features are complex: RF power is coupled on the outer of the cylinder (skin depth)
- Bfilter breaks the cylindrical symmetry: modelling is challenging

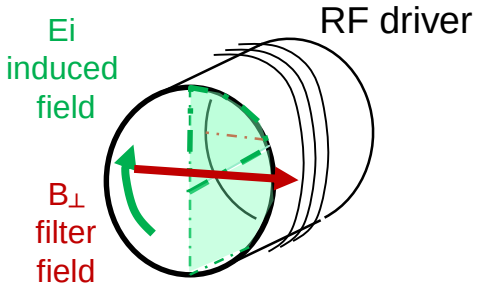

without B field, Te always peaks next to the RF coils, whatever the conductivity model; with $B_\perp$, the conductivity model determines the radial profile of absorbed power

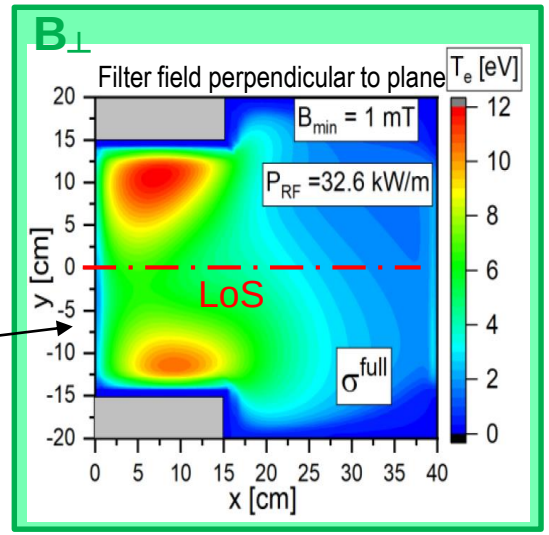

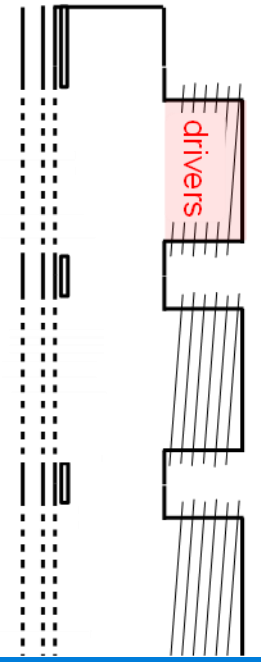

Spatial distribution inside drivers: ongoing work

- Plasma inside RF Driver features are complex: RF power is coupled on the outer of the cylinder (skin depth)
- Bfilter breaks the cylindrical symmetry: modelling is challenging

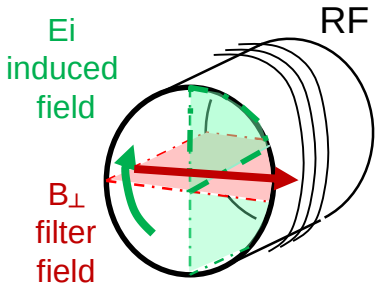

without B field, Te always peaks next to the RF coils, whatever the conductivity model; with B⊥, the conductivity model determines the radial profile of absorbed power

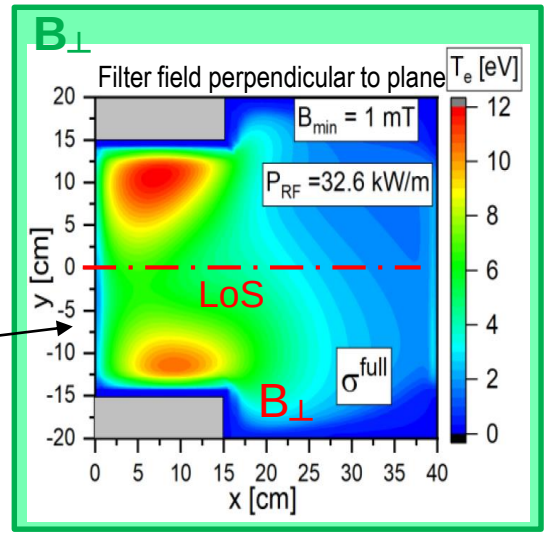

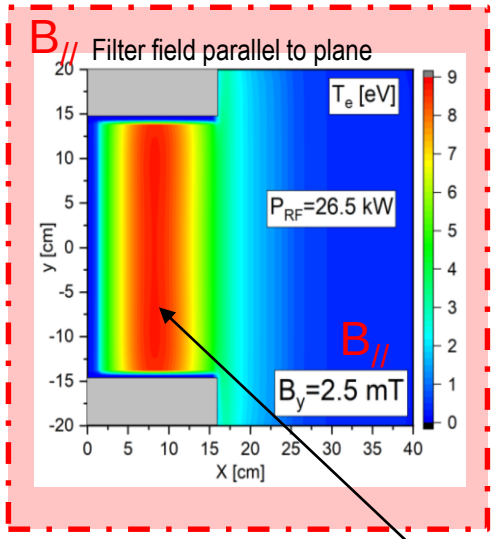

On the horizontal direction, filter field spread plasma properties horizontally

Spatial distribution inside drivers: ongoing work

- Plasma inside RF Driver features are complex: RF power is coupled on the outer of the cylinder (skin depth)
- Bfilter breaks the cylindrical symmetry: modelling is challenging
- Measurements in SPIDER aligned with smaller source, if coupling efficiency is considered
- Not the dependence on filter field

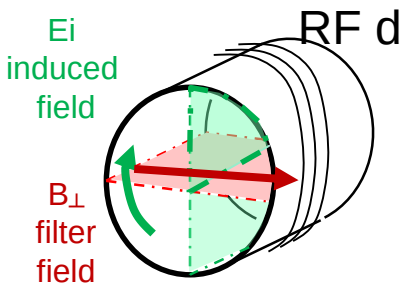

without B field, Te always peaks next to the RF coils, whatever the conductivity model; with B⊥, the conductivity model determines the radial profile of absorbed power

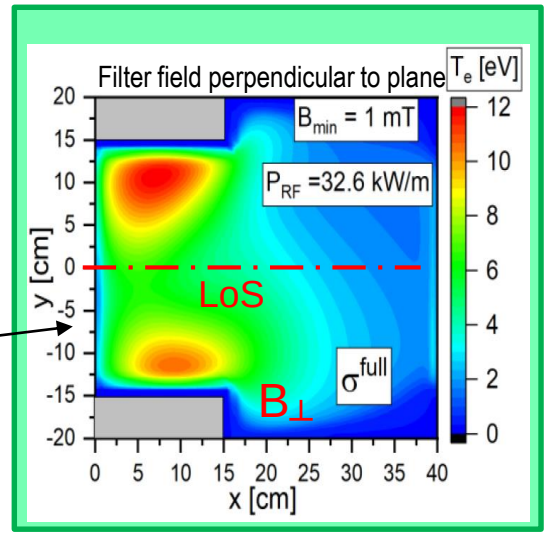

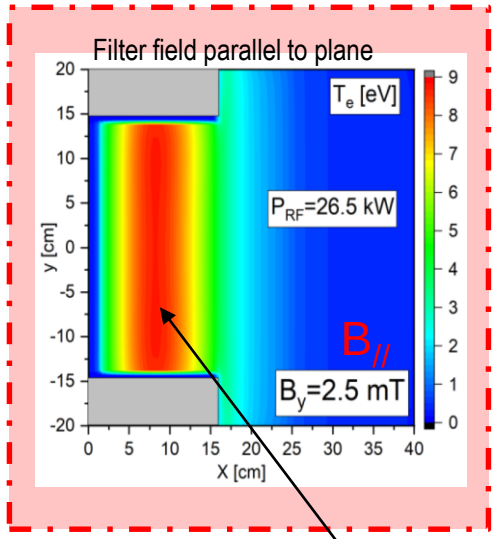

On the horizontal direction, filter field spread plasma properties horizontally

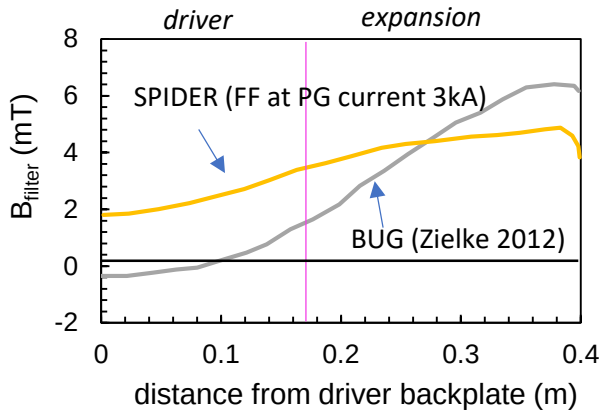

RF drivers
(view from inside the ion source)

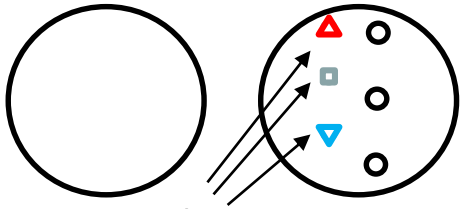

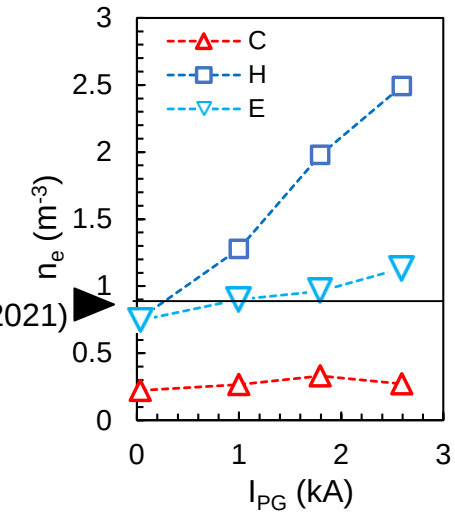

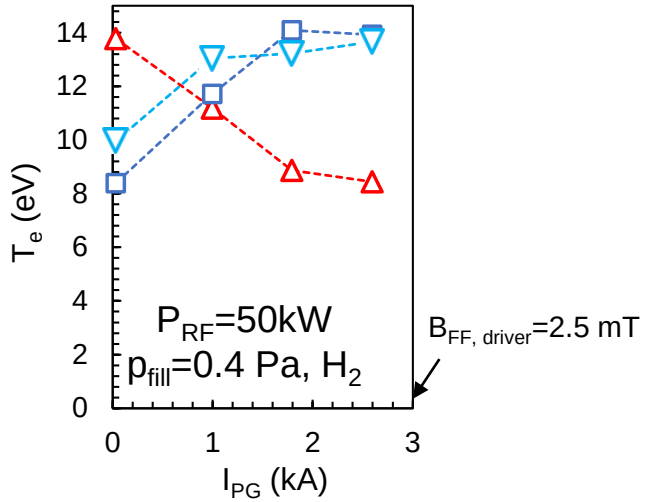

[1] Zielke J Phys D Appl Phys 54 (2021)
[2] R Zagórski, IEEE TPS 2022
[3] R Zagórski, SOFT 2022

Spatial distribution inside drivers: ongoing work

- Depletion mainly influences electron temperature, and dissociation fraction determines the ionic species H+, H2+, H3+. Neutral dynamics also determines the spatial distribution of plasma parameters [1]

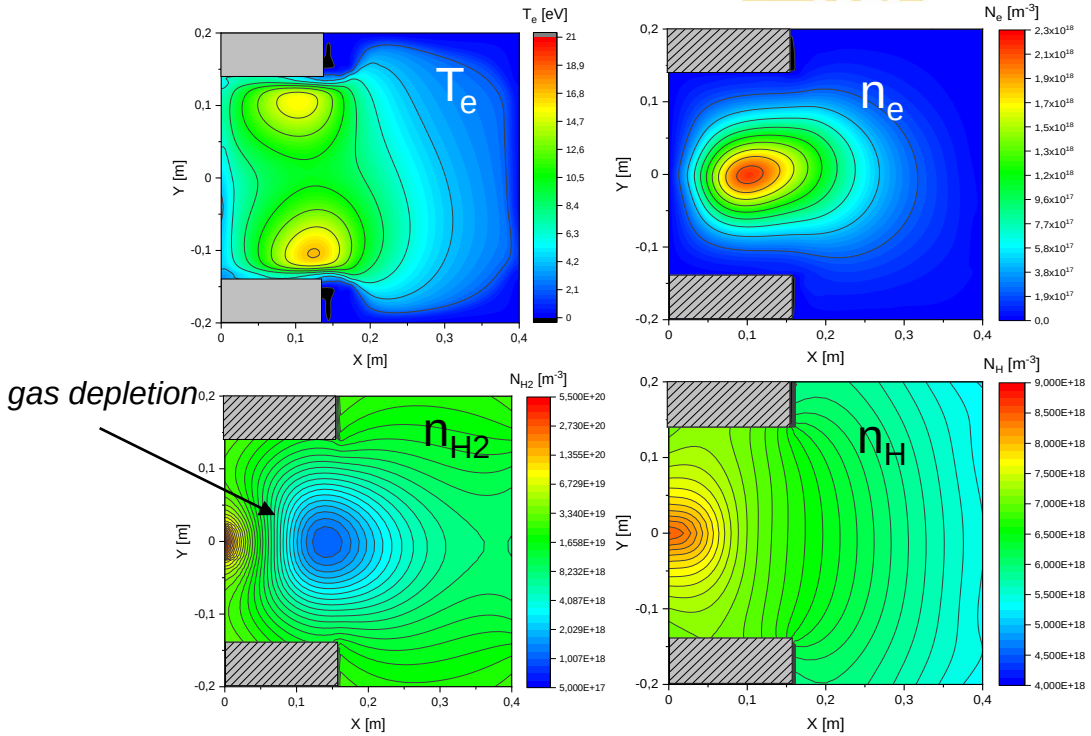

Spatial distribution inside drivers: ongoing work

- Depletion mainly influences electron temperature, and dissociation fraction determines the ionic species H+, H2+, H3+. Neutral dynamics also determines the spatial distribution of plasma parameters [1]
- via application of collisional radiative models [2,3] we obtain data on neutrals
- preliminary results in good agreement w/ probe data but also with BUG results
  important topic of collaboration

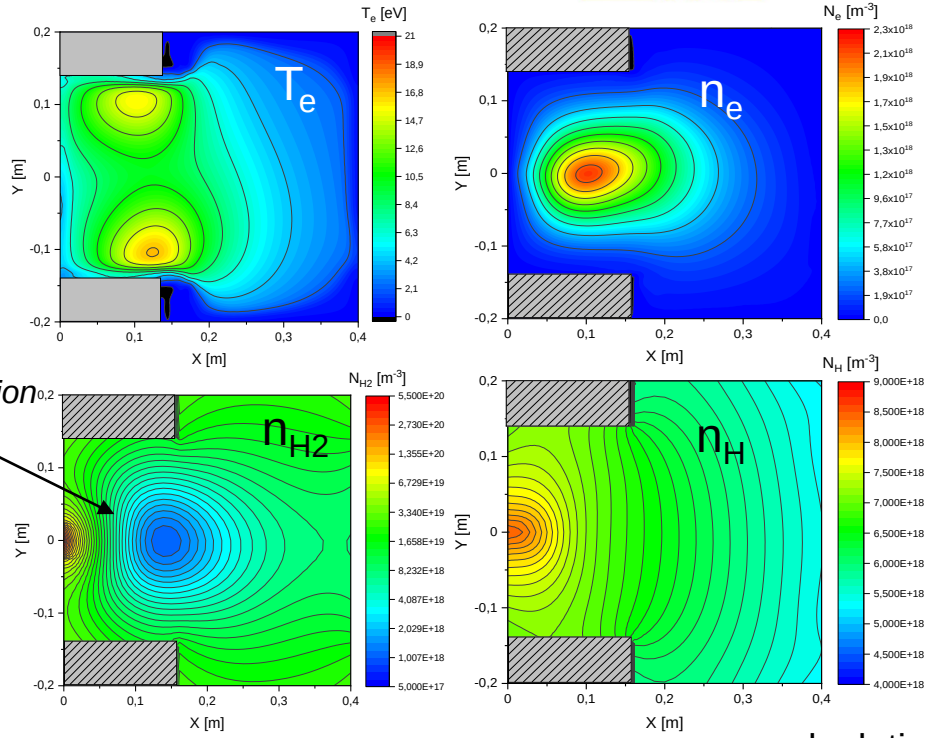

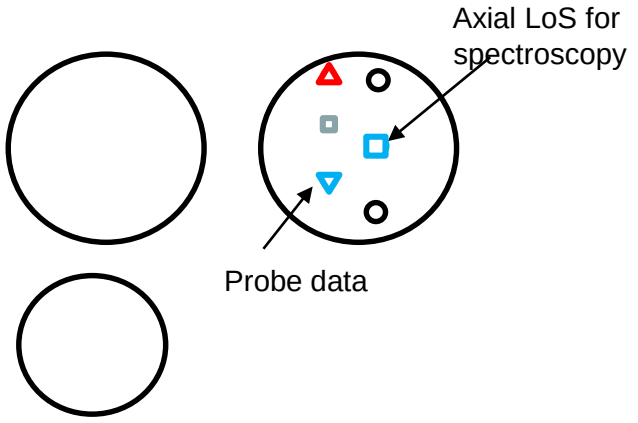

(BUG driver smaller diameter 0.23 m)

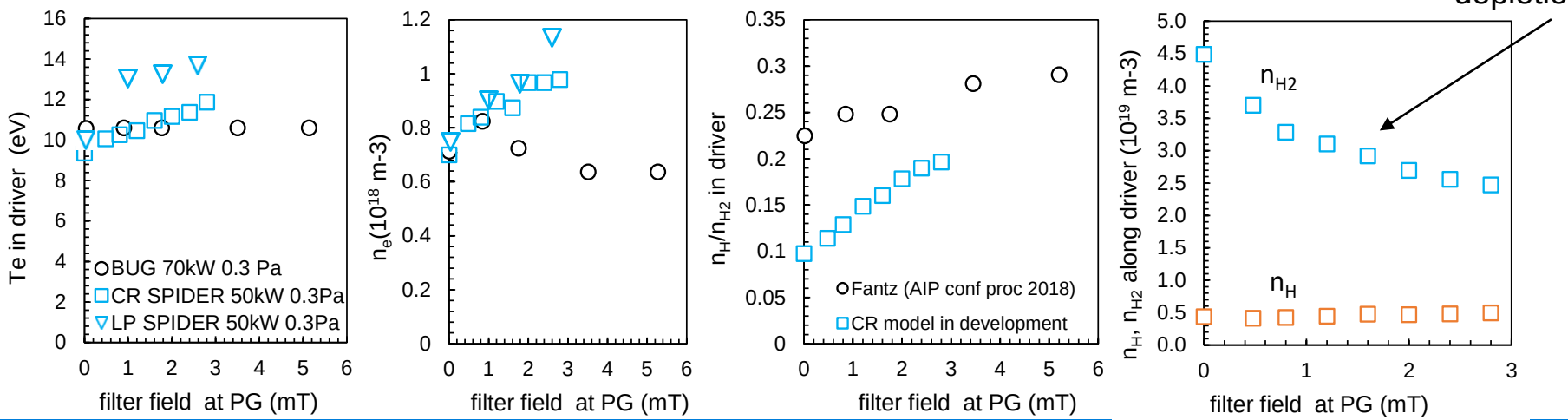

[1] Zagorski, ISFNT conference 2023
[2] Fantz AIP conf proc 2018
[2] Zaniol, Bruno

OUTLINE

- plasma parameters at the extraction region of SPIDER
- plasma parameters along expansion and driver regions in SPIDER
- positive ion energy distribution on PG in fiament arc and RF-driven sources

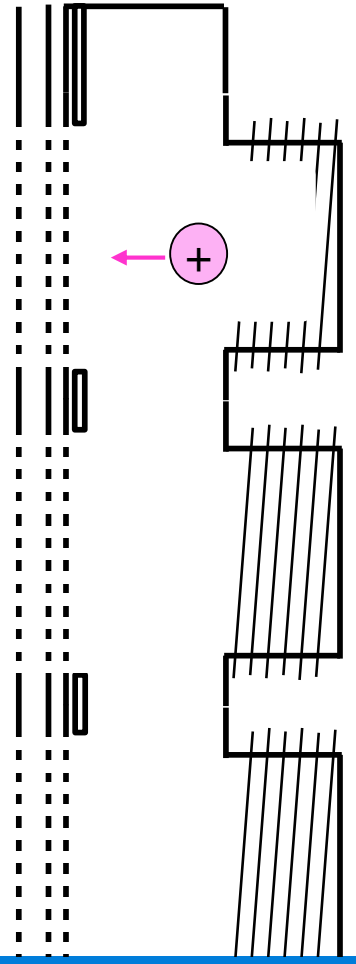

Role of positive ions

- Positive ion energy distribution $(IEDF)_z$ perpendicular to the plasma grid
- Measured by compact 4-gridded Retarding Field Energy Analysers

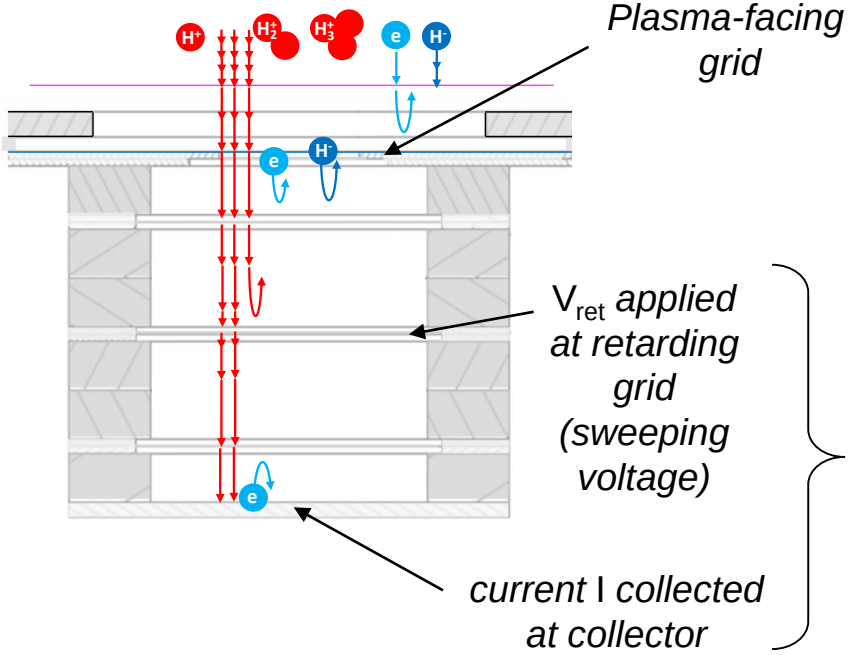

Current-Voltage characteristics $I_{coll}(V_{ret})$

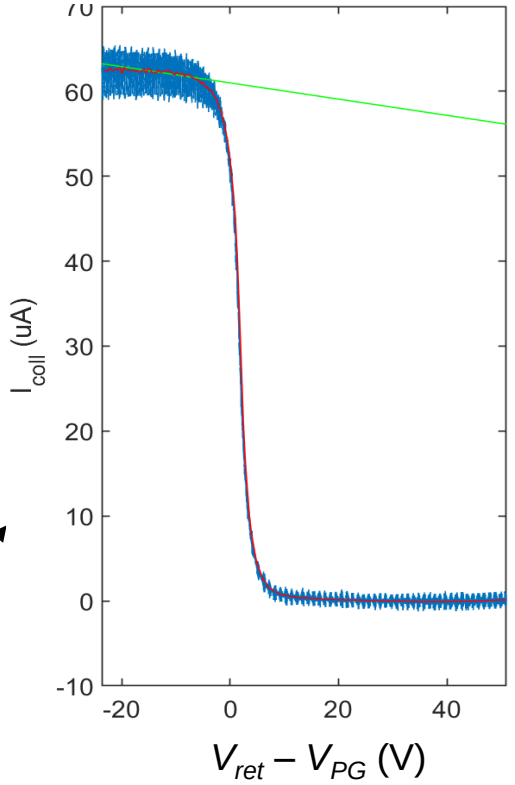

Derivative provides IEDF

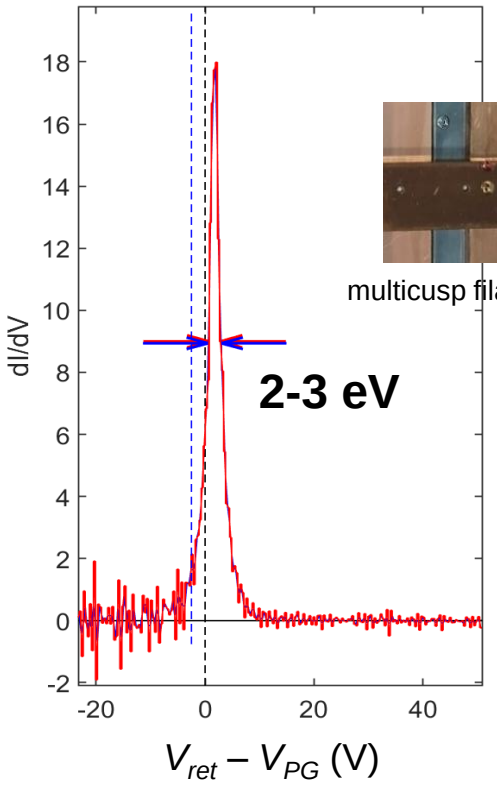

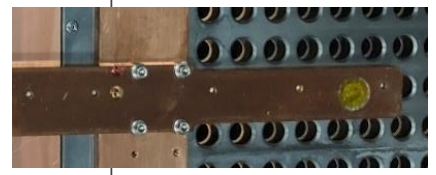

multicusp filament arc source @ NIFS

Role of positive ions

- Positive ion energy distribution $(IEDF)_z$ perpendicular to the plasma grid
- Measured by compact 4-gridded Retarding Field Energy Analysers

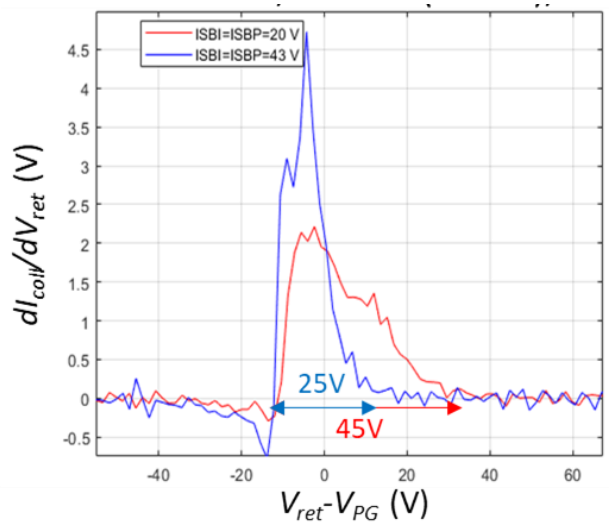

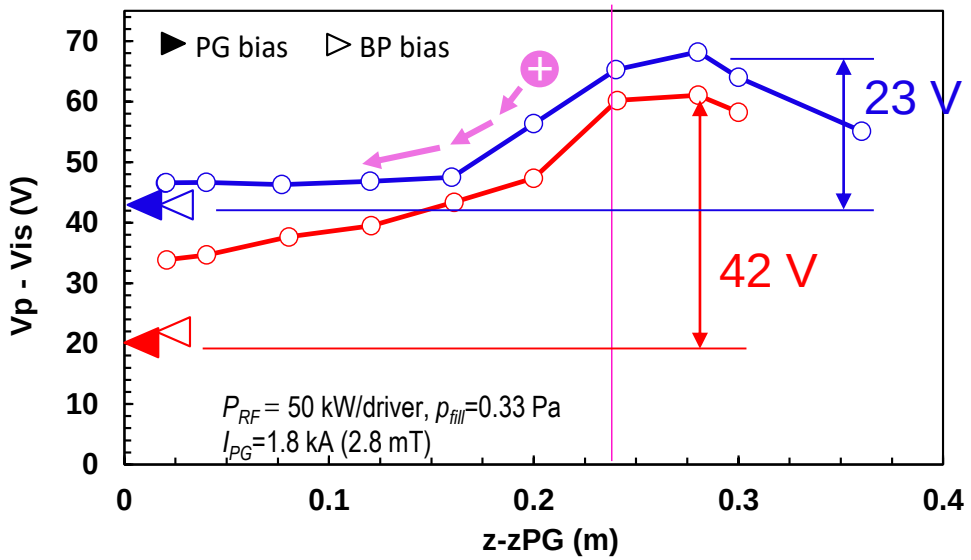

Role of positive ions

- Positive ion energy distribution (IEDF) perpendicular to the plasma grid
- Measured by compact four gridded Retarding Field Energy Analysers
- Quite good agreement between different diagnostics and different RF sources

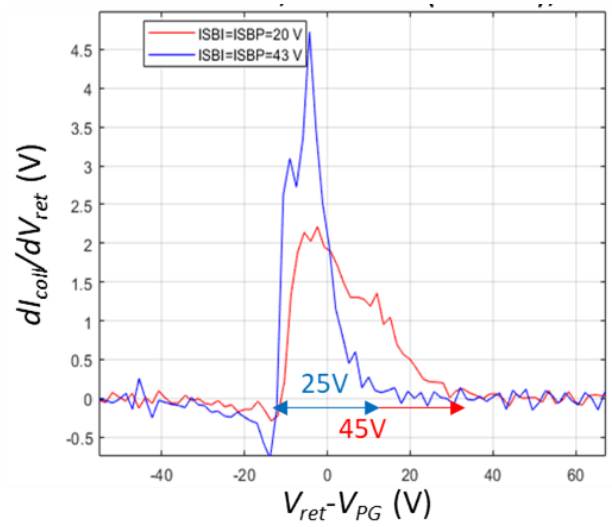

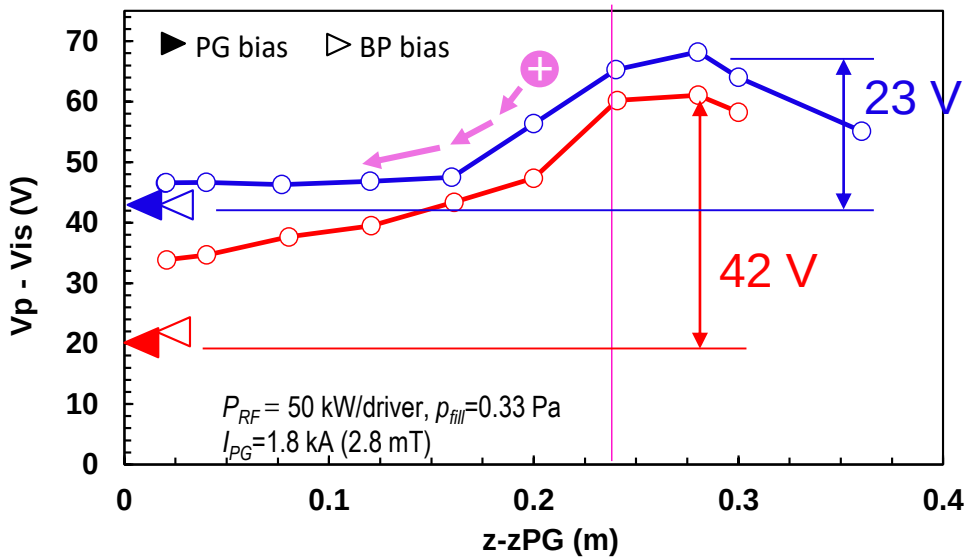

SPIDER FF=1.8 kA, U_{bias}=20V, D_2

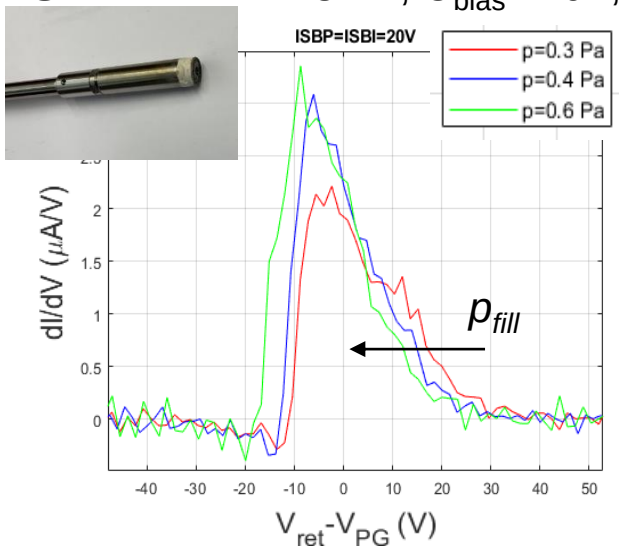

BUG FF=1.5kA, U_{bias}≈25V, H_2

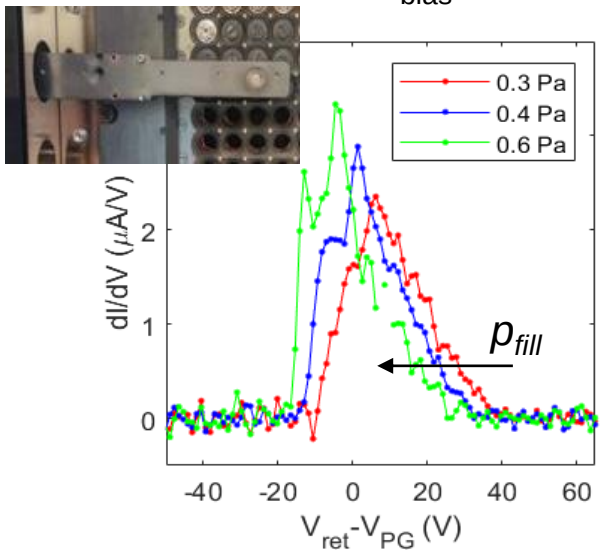

BUG FF=1.5kA, H_2

RFEA with improved resolution

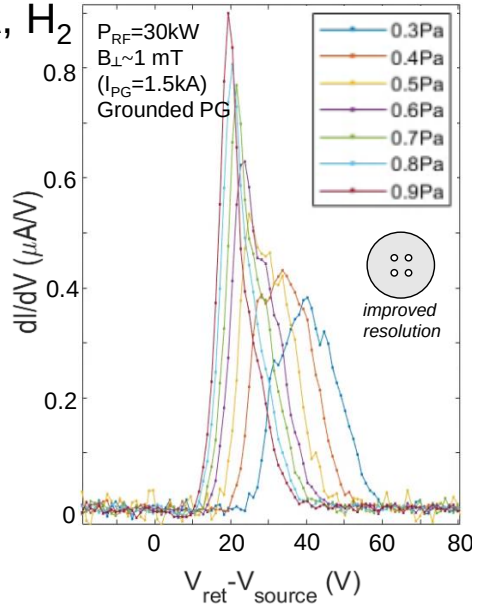

Summary and perspectives

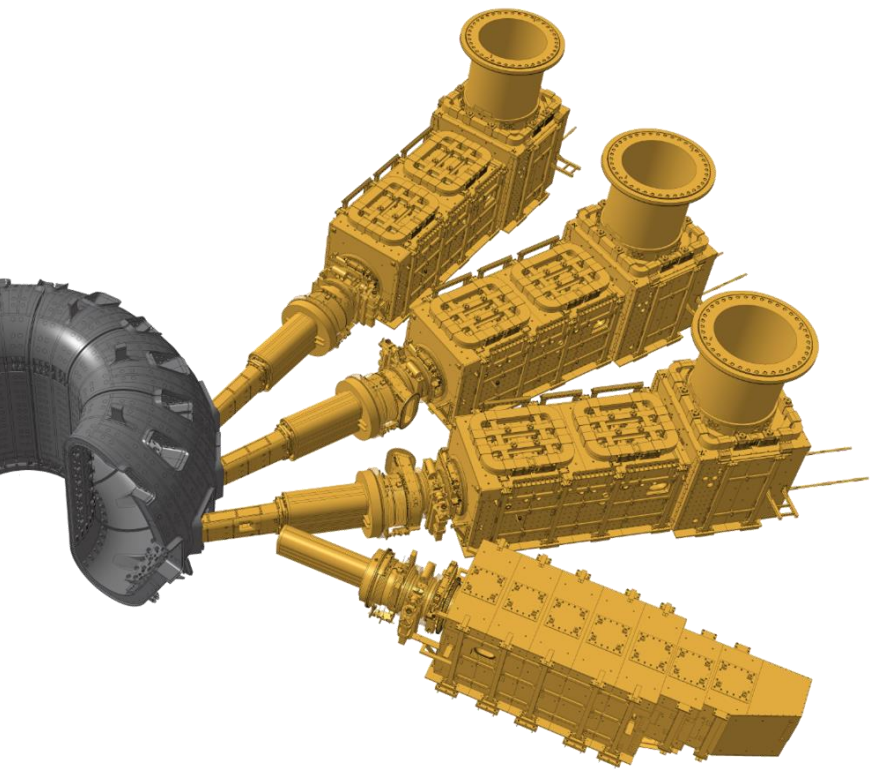

- Plasma parameters in the full scale ion source of the ITER HNB are **in line with ELISE** and smaller RF sources, of similar design
- In view of the future operations of ITER HNB, the RF driven source will provide adequate for J_ and divergence, but the margin is tight (and eroded by nonuniformities): investigation of the ion source is necessary to identify solutions to **decrease divergence** and to **mitigate non-uniformities** thus providing margin needed for a reliable operation.

Summary and perspectives

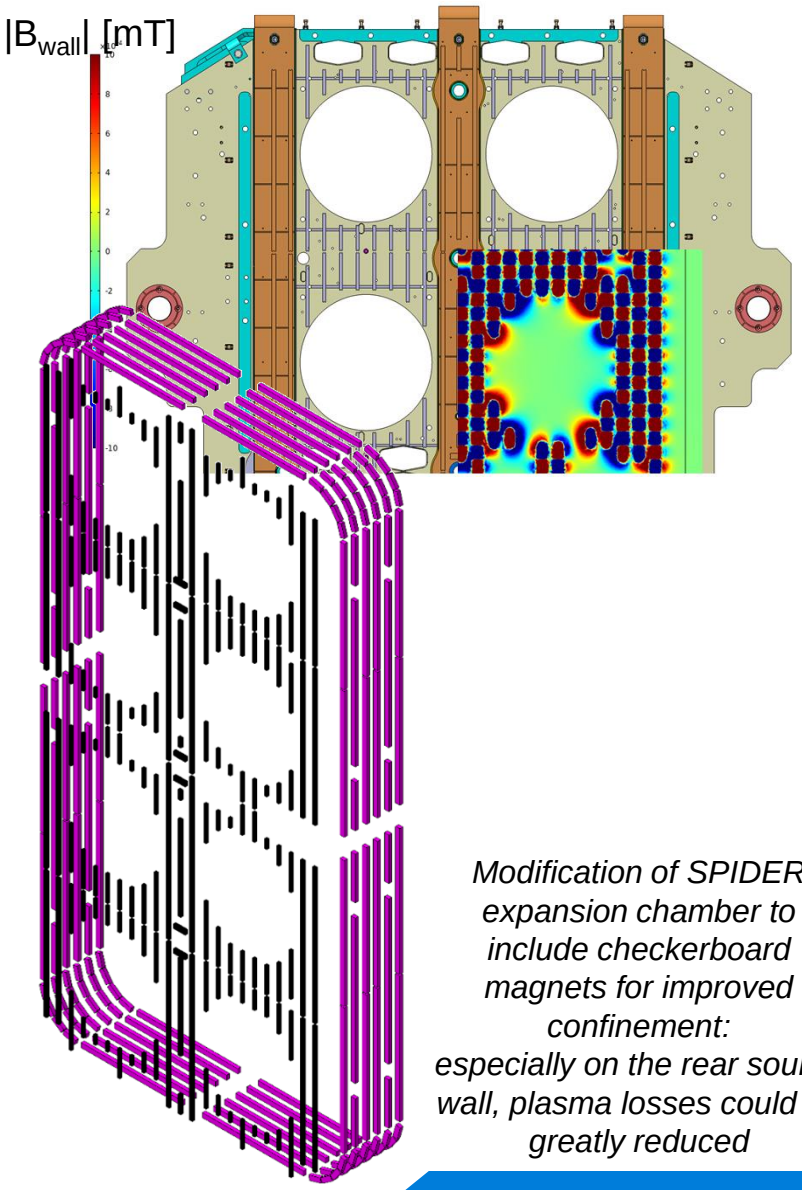

Modification of SPIDER expansion chamber to include checkerboard magnets for improved confinement: especially on the rear source wall, plasma losses could be greatly reduced

- Plasma parameters in the full scale ion source of the ITER HNB are **in line with ELISE** and smaller RF sources, of similar design
- In view of the future operations of ITER HNB, the RF driven source will provide adequate for J_ and divergence, but the margin is tight (and eroded by nonuniformities): investigation of the ion source is necessary to identify solutions to **decrease divergence** and to **mitigate non-uniformities** thus providing margin needed for a reliable operation.
- issues are shared with **giant sources of LHD and JT60SA**, such as uniformity of the plasma at the extraction region. From the highly refined plasma parameters of multi-cusp filament arc sources, we can identify **paths for improvements**. Investigation of their plasma parameters is necessary also with modelling.

SPARE SLIDES

SPIDER full-size prototype source for ITER HNB

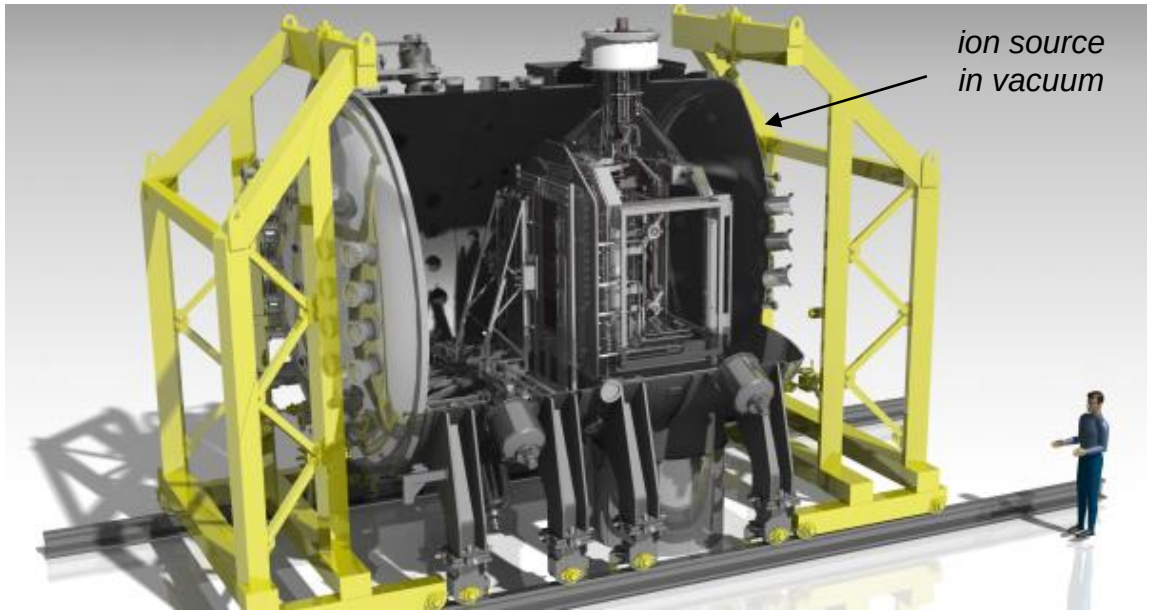

Full scale **plasma source** of ITER Heating Neutral Beams;
RF plasma source based on IPP design, 2x ELISE

Targets: optimisation of

- Extracted current density (355 A/m^2 H$^-$, 285 A/m^2 D$^-$)
- Uniformity over 1280 apertures (within 10%)
- Stability (1 h beam)
- Co-extracted electron fraction (<0.5 H$^-$, <1 D$^-$)

first plasma

influence of vessel pressure on RF discharges clarified

first extracted beam, masking most extraction apertures

source plasma studied with movable probes

Improving availability and reliability [1h/day plasma on]

HV >30kV available

First operation with caesium

shutdown for improvements

2018 2019 2020 2021 2022

AIM OF THIS PRESENTATION:
Discuss how to improve SPIDER beam parameters using experimental results obtained so far

- Axial profiles measured with RF compensated with ϕ 8mm probes[1]
- Plasma potential could not be measured directly all along the profile

$$V_p - V_f \approx \mathrm{T_e} \ln\left(\frac{A_e}{A_+}\sqrt{\frac{m_+}{2\pi\, m_e}}\right)$$

- electrons are magnetised in the expansion region, $\nu_{g,e} \sim 10 \cdot \nu_{m,e}$
- with dimensionless magnetic field strength $\beta \approx r_{pr} e|\bar{B}|/\sqrt{m_e e \mathrm{T_e}}$
- the ratio of collection areas can be estimated [2]

$$\frac{A_e}{A_+} = \frac{A_\perp\left(1-\exp\left(-\frac{\beta^2}{2}\right)\right)+A_{pr}\exp\left(-\frac{\beta^2}{2}\right)}{A_{pr}}$$

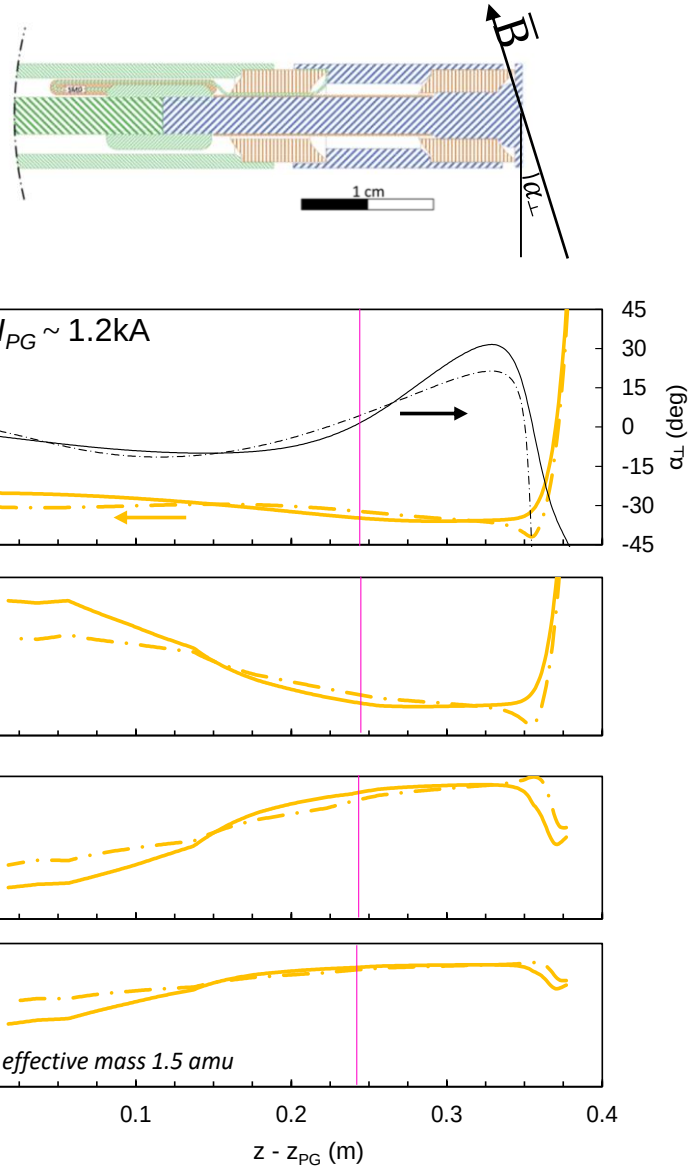

[1] E Sartori, et al., Fus Eng Des 169, 112424 (2021)
[2] M Usoltceva, et al., Physics of Plasmas 25, 063518 (2018); doi: 10.1063/1.5028267

Negative ions

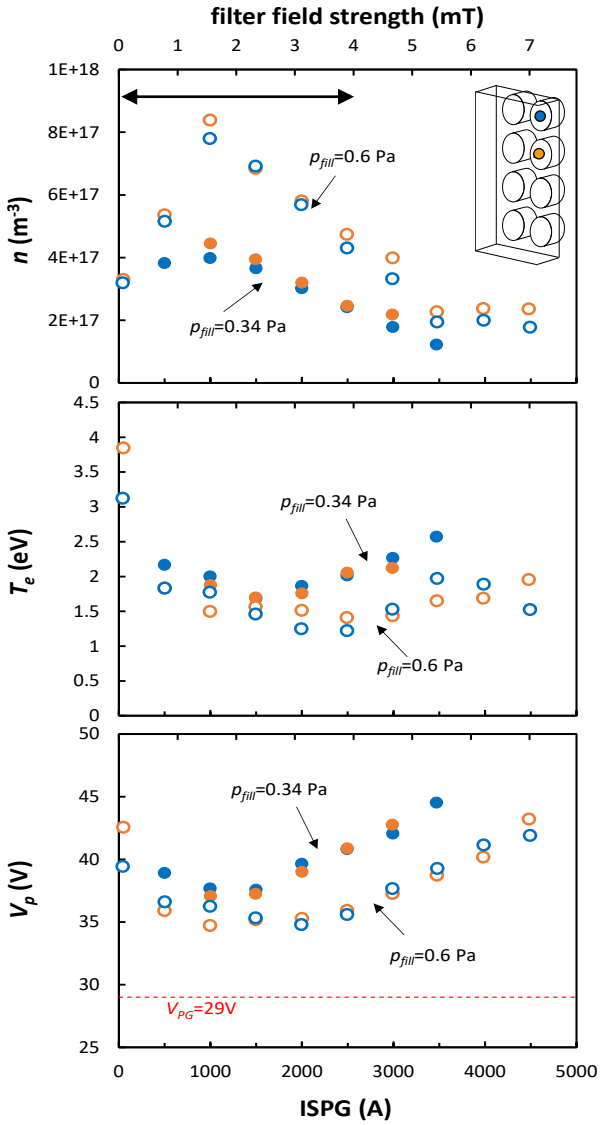

[1]

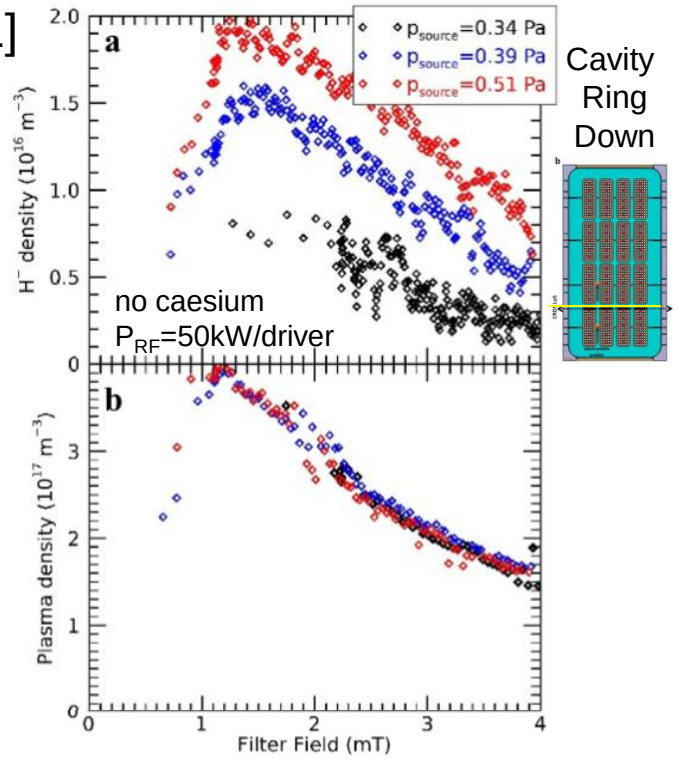

[2]

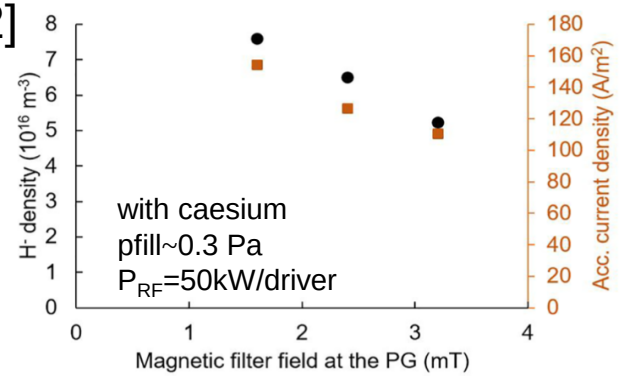

- Filter field influences the negative ion density both in volume or caesium operation [1,2]
- Also with caesium, achieve a sufficiently high positive ion density is necessary to compensate the space charge of negative ions, and allow their extraction from the converter surface

[1] M Barbisan PPCF 2022
[2] M Barbisan FED 2023
[3] U Fantz, et al., Front. Phys. 9:709651 (2021)